International Journal of Nanomedicine

Dovepress
open access to scientific and medical research

Open Access Full Text Article

REVIEW

Advancement of Electrospun Nerve Conduit for Peripheral Nerve Regeneration: A Systematic Review (2016–2021)

Shin Yee Lee[1], Soon Yong Thow[2], Shalimar Abdullah[2], Min Hwei Ng[1], Nor Hazla Mohamed Haflah[2]

[1]Centre of Tissue Engineering and Regenerative Medicine, Faculty of Medicine, Universiti Kebangsaan Malaysia, Cheras, Kuala Lumpur; [2]Department of Orthopedics and Traumatology, Faculty of Medicine, Universiti Kebangsaan Malaysia, Cheras, Kuala Lumpur

Correspondence: Nor Hazla Mohamed Haflah, Department of Orthopedic & Traumatology's Faculty of Medicine, UKM, Cheras, Kuala Lumpur, Tel +6012-3031316, Email hazla1971@yahoo.com

Abstract: Peripheral nerve injury (PNI) is a worldwide problem which hugely affects the quality of patients' life. Nerve conduits are now the alternative for treatment of PNI to mimic the gold standard, autologous nerve graft. In that case, with the advantages of electrospun micro- or nano-fibers nerve conduit, the peripheral nerve growth can be escalated, in a better way. In this systematic review, we focused on 39 preclinical studies of electrospun nerve conduit, which include the in vitro and in vivo evaluation from animal peripheral nerve defect models, to provide an update on the progress of the development of electrospun nerve conduit over the last 5 years (2016–2021). The physical characteristics, biocompatibility, functional and morphological outcomes of nerve conduits from different studies would be compared, to give a better strategy for treatment of PNI.

Keywords: electrospun nerve conduit, in vivo, peripheral nerve regeneration, scaffold, animal defect model

Introduction

Peripheral nerve injury (PNI) is a worldwide problem which hugely affects the quality of patients' life. As a consequence of the injuries, patients often suffer painful neuropathies with reduction in motor function and sensory perception.[1] In severe situations, the nerve is completely ruptured, resulting in a gap, necessitating surgical procedures to restore nerve functionality.[2] Currently, there are different surgical procedures available, including end-to-end suture which is preferably used in short nerve gaps (<5 mm).[3] In larger nerve gaps, an autologous nerve graft procedure is currently the gold standard[4] despite its limitations, such as additional surgery, scarring and donor-site morbidity, and limited source of donor nerves.[5] Thus, there is a strong need to find innovative therapies for treatment of PNI.

There are alternative nerve conduits available on the market to mimic autologous nerve graft, which are made of synthetic polymers such as collagen, PLGA, silicone; or decellularized nerves. Decellularized nerves are obtained from the human dead body, decellularized, retaining some extracellular matrix-related protein. They are cleaned of their antigenic component yet retain their 3D structure which serves as scaffolds for axonal growth.[6] Although the decellularized nerve graft has been rated as the next best procedure for PNI treatment, it has limitations such as its source from a dead body and its expensive price (around RM 15k–20k). This has led to the further research of nerve conduits using synthetic polymers, which are cheaper and easily obtained. Therefore, the search for an ideal nerve conduit is necessary to replace autologous nerve graft in a similar effectiveness, with longer length and additional biological additives such as cell-seeded nerve conduit or neurotrophic factors-/drugs-/bio-functional peptides-added nerve conduit.

There are many techniques that can be used to fabricate nerve guidance conduits. In comparison to other methods, electrospinning is relatively easy and less labor intensive.[7,8] This review will focus on electrospun nerve conduits due to the numerous advantages of the electrospinning technique. Electrospinning produces randomly or aligned fibrous mats with fiber diameters ranging from nanometers to micrometers. This technique allows the use of different synthetic and

Received: 14 February 2022
Accepted: 5 November 2022
Published: 28 December 2022

natural polymers and results in three-dimensional fibrous microstructures capable of mimicking the native extracellular matrix (ECM). Moreover, electrospinning meets the requirement of porous and flexible mats that have a high surface area to sufficiently enhance cell–substrate interactions.[9] Physically and linearly guiding axon growth increases the probability of functional recovery of the injured nerve.[10] The use of electrospun conduits with an aligned structure has advantages over the commercial hollow tube conduits, such as high porosity, high specific surface area which increases the area available for protein absorption, Schwann cell migration and axon regeneration. Additionally, aligned nanofibers promote cell proliferation and growth, and guided axonal growth,[1,11] preventing the formation of neuroma.

The objective of our study is firstly, to provide an update on the progress of electrospun nerve conduit over the last 5 years (2016–2021). Secondly, is to gather and review all preclinical and clinical data on electrospun nerve conduit to date.

Materials and Methods

Keywords Used

The following keywords were being used for searching literatures through databases:

"nerve tissue engineering" OR "tissue-engineered nerve" OR "nerve conduit" OR "nerve guidance conduit" OR "nerve scaffold" OR "tissue scaffold" AND "in vivo nerve regeneration" OR "peripheral nerve regeneration" OR "nerve regeneration" AND "electrospun nanofiber" OR "electrospun nanofibers" OR "electrospinning nanofiber" OR "electrospinning nanofibers" AND "transplantation" OR "cell transplantation" OR "cells transplantation".

Selection Process and Data Extraction

The following databases were being used for searching literatures for this study: PubMed database, Scopus database, Science Direct database and Ovid database. After searching by the keywords above, the results were further filtered by years (2016–2021), language (English) and article type (only research articles were included). After applying those filters, each article or literature was included based on their: title, which stated "nerve conduit", "in vivo" or "nerve regeneration"; abstract, which mentioned "electrospinning nerve conduit", "in vivo study" or "animal defect model"; and method, which clearly listed the procedures and protocols of fabrication of electrospun nerve guidance conduit or animal surgery, to ensure the articles were related to "electrospun nerve conduit for peripheral nerve regeneration".

The screening of the research articles was performed by two reviewers (SYL and MHN). Any disagreement during the screening process were resolved through discussion between the two reviewers. Relevant information from the selected articles were extracted and documented in the data extraction sheet (Figure 1).

Results and Discussion

Selection of Articles

According to the keywords and criterion above, there are 39 literatures in total that were included in this study, which could be further categorized by the 4 varieties of nerve conduit. The yields of each category are as follows: 18 for nerve conduit with nanofibers only,[12–29] 6 for nerve conduit with cells seeded,[30–35] 12 for nerve conduit with additional factors (neurotrophic factors, drugs and bio-functional peptides)[36–49] and 3 for nerve conduit with the combination of cells seeded and additional factors.[48–50]

Study Characteristics

In this study, the data and information extracted were tabulated and included the review of material used as nerve conduit, their properties and their in vitro biocompatibility, the additional factors incorporated such as cells and non-cellular factors, and the functional and morphological assessment of in vivo implantation of the nerve conduit will be presented as Table of Comparison, which are shown as Tables 1–5 as follows.

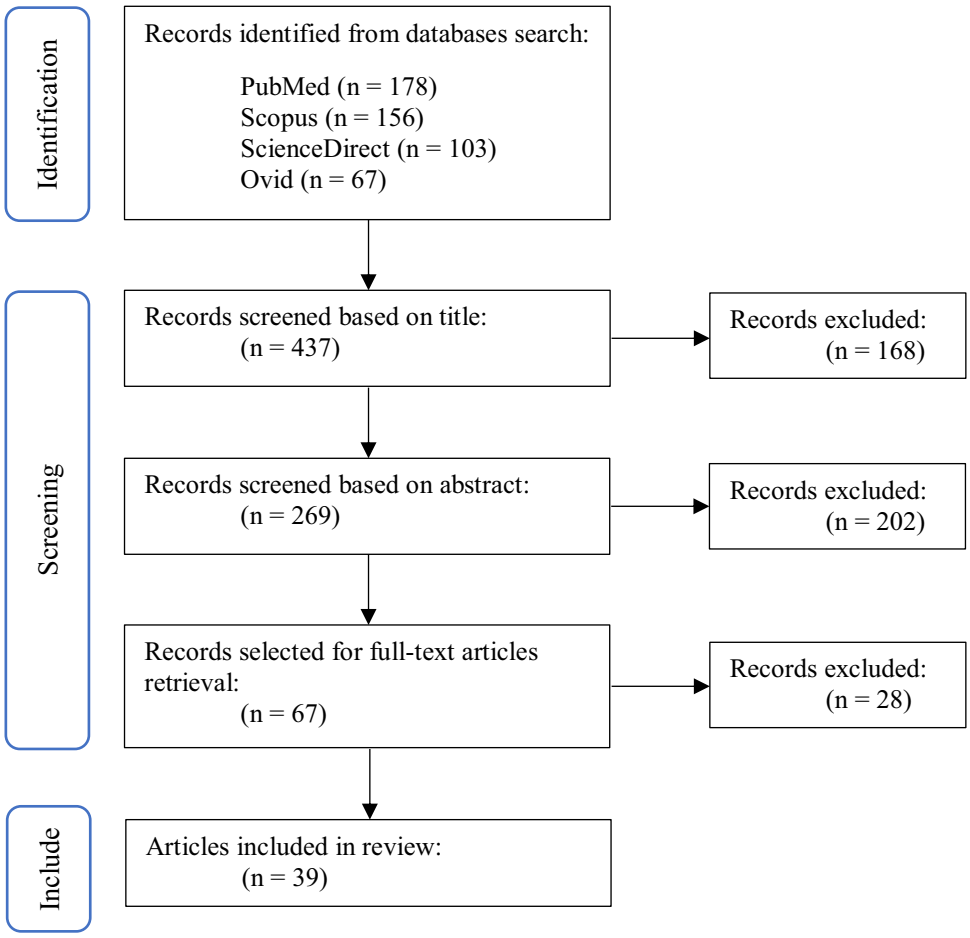

Figure 1 Flowchart for the identification and selection of studies.

Nerve Conduit Materials

Fabrication Method

The electrospinning techniques that were used for nerve conduit fabrication included classic electrospinning and coaxial electrospinning. The classic electrospinning only allows one ejection of one polymer solution at one time, while coaxial electrospinning allows two polymer solutions to be ejected at the same time, resulting in nano- or micro-fibers with a "core/shell" structure. Core and shell represent the inner layer and outer layer of a nerve conduit respectively. Thus, the different structures of nerve conduit fabricated by different electrospinning techniques could be classified as: single layer of fibers or core/shell layers of fibers. Moreover, not only the "hollow" nerve conduit that consists of only layers of fibers (with nothing added in the lumen of conduit), but also the nerve conduit that is filled with freeze-drying nano-sponge (NS) or hydrogel (in the lumen) could be used as the scaffold for peripheral nerve regeneration study.

Material Used

According to Table 1, there are various types of materials that can be used for the fabrication of nerve conduit, which can be categorized to either natural, synthetic or hybrid.

Among these polymers, PCL, with its ease of processability, mechanical strength and proper stability under ambient conditions,[51] is the most popular polymer to be used in studies from year 2017 onwards. Its usage continues to increase in the later years either independently, or incorporated with gelatin, PLGA, CNF, CL or chitosan. Recently studies are focusing on PLLA on account of of its good biocompatibility, acceptable biodegradability and thermoplastic processability.[52] Nevertheless, in electrospinning, PLGA, gelatin and chitosan are the polymers that people are familiar with and continue to use until now.

However, PLCL, PPY, CL, PHBV and various types of silk fibroin seems to reach the "bottle neck" as they have not been used since 2019, probably due to the development of more popular polymers, PCL and PLLA.

Interestingly, there are several polymers or materials that are having specific function or characteristics, which attracted much attention by researchers, such as: PFTBA which could provide short term oxygen supply to Schwann cells (SCs) and counteract the detrimental effects of hypoxia on SCs during the early stages of nerve injury;[53] PLATMC, a kind of shape memory polymer, which can realize shape recovery through an entanglement of the molecular chains without chemical and physical cross-linking;[54] and MAP that displays negative charge that can confer cell adhesion, cell proliferation and tissue regeneration due to its unique adhesive property and biocompatibility.[55]

Characteristics of Nerve Conduit

The average diameter of electrospun micro- or nano-fiber is the most important factor that concerns researchers. The diameter of electrospun fiber should be similar with or close to that of native epineurium which is 67 ± 25 nm.[29] Among the 39 studies, Niu et al[28] using PLLA and gelatin produced nano-fibers closest to the native value with the average diameter of 77 ± 35 nm. Neshat et al[24] produced the nano-fibers with average diameter 71 ± 14 nm, by adopting PCL & DSC cross-linked sodium alginate. Cheong et al[42] produced the lowest diameter nano-fibers that could be electrospun, 20–30 nm, by adopting PLGA (75:25) and 10% MAP.

The mechanical properties of a native nerve or a nerve conduit can be expressed as tensile strength, Young's modulus, elongation at break and elasticity. Tensile strength and Young's modulus are the more common indicators. The tensile strength and Young's modulus value of a native sciatic nerve of rats are approximately 6.5–11.7 MPa and 0.58 MPa respectively.[56] By comparing the data of mechanical properties of nerve conduit in Table 1, only 6 out of 39 studies have fabricated a nerve conduit having the similar mechanical properties with the native sciatic nerve: Chang et al[37] (2017; PEO/gelatin), Jing et al[18] (2018; PLGA/PPY), Wang et al[25] (2020; PLATMC), Chen et al[45] (2020; PCL), Amini et al[46] (2020; PCL) and Samadian et al[47] (2020; PCL/gelatin). We can conclude that recent studies have been more successful in developing nerve conduits which have mechanical properties closer to native nerve. The key polymer used was PCL which could account for its popularity.

It was found that conductivity is not a necessary characteristic for nerve conduit, thus, only studies that used conductive materials presented the need to test conductivity. Conductive materials such as PPY and carbon nanotubes (CNTs) are commonly used, owing to their excellent electrical properties and biocompatibility (Table 1).[57] As electrical signals might be generated between the neural cells themselves during the nerve regeneration process, electrospun conductive conduits may have the potential to propagate these electrical stimuli, and consequently, stimulate nerve regeneration.[58] However, the necessity and feasibility of conductive material for a nerve conduit graft should be further validated through the results of in vivo implantation in an animal nerve defect model, which will be discussed later.

A nerve conduit could be said as the "bridge" to connect the nerve gap and provide topological support for axonal outgrowth or cell proliferation and attachment, thus the incorruptibility of scaffold before the nerve regeneration has completed is extremely important. It is known that the nerve regeneration rate for human nerve is 1–3 mm per day, and slightly faster in rat.[59] As a result, the degradation rate of a nerve conduit should be as long as possible in order to provide enough support for axonal outgrowth through the defect nerve gap. For instance, a nerve conduit should ideally maintain its scaffold for 5 days to provide enough support for a 5 mm nerve defect model. Studies often use the weight loss percentage or swelling ratio after immersing the scaffold into normal saline or PBS in vitro over a period of time to express the degradation rate of the scaffold. Alternatively, some studies after implanting the scaffold subcutaneously over a period of time roughly estimate the percentage of degradation by gross observation. However, gross observation or simply weighing are not absolute to the cell environment. For example, if small corruptions had happened inside the lumen of scaffold, it might be a critical situation for cells in the scaffold even if no obvious degradation could be observed. Therefore, we should evaluate the degradation rate of scaffold in detail using a microscope in order to effectively express the situation of cells, but none of the 39 studies have done the evaluation under a microscope.

The biocompatibility of nerve conduit is the key indicator for in vivo implantation. An in vitro evaluation of nerve conduit with actual cells is necessary before having implantation to assess survival and viability of cells after seeding onto fabricated nerve conduit. Six studies did not evaluate in vitro biocompatibility (Table 1). Cells used by the other

Table 1 Comparison of the Fabrication Method, Material Used and Characterization (Including Biocompatibility) of Nerve Conduit

Ref.	Scaffold Materials and Alignment (Shell/Core)	Electrospinning Parameters	Characterization							
			Fiber Diameter	Mechanical Properties	Conductivity	Pore Size (μm)	Porosity (%)	Degradation / Swelling	Surface Hydro-Philicity (WCA)	(In vitro Cell Line) Biocompatibility
Nerve Conduit with Micro- or Nano-Fiber Only										
Zhou Z. F. et al (2016)[12]	(11 mm L) PELA-PPY^{r} (20%)	0.2 mm diam. needle; 20 kV; 1 mL/h; rotating rod (2 mm diam.) 300 rpm; 15-cm distance	Ave. diam.: 503 nm	Ave. fracture stress: 7.8 MPa; 49.8% max. tensile strain, declines to 17.0%	Too low to be measured	–	–	–	–	(Rat adrenal PC12 cells) Cells attach & proliferate well
Song et al (2016)[13]	(2 mm Φ) PPY-PLCL^{r}	1 mL/h; 12 kV; 50 rpm	Ave. diam.: 805.6 ± 152.1 nm	–	6.72 x 10^{-5} S/cm	–	–	(in vivo) Obvious degradation at 8 weeks	–	(PC12 cells) (DRG cell lines) Electrical stimulation significantly elevated the median neurite length
Zhang et al (2016)[14]	(Φ: inner 1.5 mm, outer 2.0–2.3 mm) PLGA-SF-CL^{r}	12 G needle; 20 kV; 15 cm distance; 2 mL/h; 2000 r/min	Diam.: 300–500 nm	Tensile strength (MPa): 2.45 ± 0.33 (outer), 1.96 ± 0.34 (inner)	–	–	90.2 ± 0.8 (outer), 87.3 ± 0.6 (inner)	–	–	–
J. Du et al (2017)[15]	Chitosan/ fibrin hydrogel^{a}	0.5 mm diam. needle; 5 kV; 3 mL/h; rotating collector (50 rpm)	SEM reveals linearly ordered fibrin hydrogel within chitosan conduit	Elasticity: ~1.5 kPa	–	–	–	–	–	(SCs, DRGs from rats) Cells elongate along long axis of fibers
Sun B.B. et al (2017)[16]	(10-mm L) PLCL^{r}-SF nanofiber membrane^{a}/ nano-sponge (NS)	21G needle; 12 kV; 1 mL/h; 5–6 cm distance; Freeze-drying; Cross-linked via glutaraldehyde vapor	Ave. diam.: 975.51 ± 78.21 nm (inner), 987.38 ± 102.01 nm (outer); NGC: 2-mm	Max. stress: 376.93→292.65 kPa; Young's modulus: 28.48→13.27 kPa	–	0.5–12 (outer), 1–100 (inner)	72.84 ± 2.93 (outer), 88.81 ± 1.13 (inner)	–	–	(SCs from rats) Showed good viability & infiltrate into sponges
X.F. Zhang et al (2018)[17]	(12 mm L, 2 mm inner Φ) PHBV-PEO^{a} (6:1)	No. 6 needle; 12 kV; 5 mL/h; 25 cm distance; roller (6 cm Φ, 8 cm ι)	Ave. diam.: 787 nm; PEO increase, diam. increase	–	–	–	–	–	–	(RSC 96 cell line) Good cellular compatibility
W. Jing et al (2018)[18]	(12 mm L) PLGA-PPY (PP^{a}: outer layer; POP^{a}: inner-filled fiber)	0.5 mm needle; 20 kV; 0.6 mL/h; 20 cm distance	Diam. (nm): 783 ± 345 (PL GA), 936 ± 412 (POP); PPY surface thickness: ~150 nm	Tensile strength (MPa): 8.25 ± 1.11 (POP), 11.78 ± 1.42 (PLGA)	POP: 0.118 S/cm (1.043 x 10–5 S/cm at week 12) PPY: 0.302 S/cm, PP: 5.36×10-3 S/cm	–	–	(12 weeks) PP: ~50% weight loss, PP-POP: ~40% weight loss, PLGA: > 90% weight loss	–	(PC12 cells) Rough PPY increase degree of cell attachment; fastest cell growth rate on POP
B. Sun et al (2019)[19]	PPY-PLCL-SF^{a}	21G needle; 12 kV; PTFE stick collector (2 mm Φ, 50 mm L)	–	–	Amount of PPy coating: 25.31 ± 1.52 μg per 1 mg PLCL/SF NGC	–	–	–	–	–

(*Continued*)

https://doi.org/10.2147/IJN.S362144 DovePress

Table 1 (Continued).

Ref.	Scaffold Materials and Alignment (Shell/Core)	Electrospinning Parameters	Characterization							
			Fiber Diameter	Mechanical Properties	Conductivity	Pore Size (μm)	Porosity (%)	Degradation / Swelling	Surface Hydro-Philicity (WCA)	(In vitro Cell Line) Biocompatibility
S. Farzamfar et al (2019)[20]	PCL-CNF[f]/ PCL-collagen[a]	Freeze dried; 18G needle; 18 kV; 0.5 mL/h; 15 cm distance	Ave. diam.: 1234.48 ± 57.3 nm	–	Resistance: 8.7×10^4 ± 0.34×10^4 Ω	≈ 100	B: 82.9 ± 3.7; C: 88.5 ± 5.8	1.84 ± 0.37% (30th day), 3.58 ± 0.39 (60th day)	–	(PC12 cells) Good cell proliferation
J. Lopez et al (2019)[21]	PCL[a]	27G needle; 7.5 kV; 5 mm/s; steel mandrel (1.5 mm Φ, 30 cm L); 6 cm distance	–	–	–	–	–	–	–	–
Yen C.M. et al (2019)[22]	PCL-type I collagen[a]	21G needle; 20 kV; 2 mL/h; 20 cm distance	Diam. coeff. of variation: 12.64%; Ave. diam.: 200–300 nm	–	–	–	–	–	–	–
J. Wang et al (2019)[23]	(10-mm L, 2-mm Φ) GO-coated ApF-PLCL[r]	2 mm diam. PTFE stick	Ave. diam.: 607 ± 127 nm; GO loading %: 1.18 ± 0.04	Tensile strength: 13 MPa; Elongation at break: 160%; Young's modulus: 37 MPa	–	–	–	–	53.3 ± 1.8°	(PC12 cells, RSC 96 cell line) Significantly promoted cell growth & proliferation; Mature bipolar morphology of SCs
Neshat A. et al (2020)[24]	(15-mm L) PCL & DSC cross-linked sodium alginate (P-CA)[r]	22G needle; 14 kV; 0.2 mL/h	Ave. diam.: 71 ± 14 nm; 3–3.5 mm inner diam., 0.17–0.37 mm thickness, 14–20 mg weight	Ave. suture retention strength: 301 N/mm^2 Tensile strength: 16.95–19.65 MPa Young's modulus: 104–157 MPa; Strain at break: 35–37.5%	–	Ave.: 9.695 ± 4.346	65.72 ± 4.86	Swelling rate: 503% (8 h), reached plateau after 72 h; Degradation rate: 2.6% (1st day), 28.3% (30th day)	–	(PC12 cells) Cell viability: 95.1% (1st day), 113.4% (7th day)
J. Wang et al (2020)[25]	PLATMC[r/a] (multi-channeled, 4 smalls + 1 big: inner diam. 0.6 & 2 mm)	22G needle; 17 kV; 1.5 mL/h	Ave. diam.: 1107.97 ± 141.65 nm (LA: TMC = 70:30)	Tensile strength: 10 MPa; Elongation at break: >200%; Shape recovery process: 12s (small tubes), 25s (big tubes)	–	–	–	–	–	(PC12 cells, RSC 96 cell line) Cell viabilities > 90%; cells with spindle-like shape, elongated cell soma & longer neurite
Q. Zhang et al (2020)[26]	PLLA-SPI[a]	0.69 mm diam. needle; 12 kV; 1.2 mL/h; 11-cm distance	Diam.: 983 ± 222 nm to 349 ± 98 nm (0% to 60% SPI); ≈400 nm for SPI 20%	Stress–strain: SPI decreased ductility; Tensile strength: 1.99 ± 0.54 to 3.47 ± 0.82 MPa (0–60% SPI); Elongation at break: 26.65 ± 5.23 to 3.44 ± 0.72% (0–60% SPI)	–	–	–	(in vivo, subcutaneously implanted) SFI 20% had degradation time around 12 weeks	PSNF-20: 123.31° ± 7.73°	(PC12 cells, RSC 96 cell line) Good cytocompatibility; aligned bipolar distribution; more than 80% of cells has neurites

F. Moharrami Kasmaie et al (2021)[27]	(7 mm L) PCL-PLGA[a]	20 kV; 0.5 mL/h; 20-cm distance; 600 rpm	Diam.: 575.7 ± 22.2 (inner, PCL /PLGA), 388.5 ± 19.3 (outer, PCL); Alignment index (%): 0.97 (inner), 0.98 (outer)	–	–	–	–	–	Inner: 98.1 ± 1.6°; Outer: 110.0 ± 2.1°	(A-172 cell line) No significance difference of cell proliferation between control & scaffold group
Y. Niu et al (2021)[28]	(12 mm L) PLLA-gelatin[r] (75:25)	7.5 kV; 5 mm/s; stainless steel needle (1.26 mm Φ, 150 mm L); 150 mm distance; 1000 rpm	Ave. diam.: 77 ± 35 nm (native epineurium 67 ± 25 nm)	Effective elasticity: 3.1 ± 0.9 kPa; Tensile strength: 12.9 ± 7.8 MPa (native nerve tissue ≈ 11.7 MPa)	–	–	86.5–87.6 (native epineurium ≈ 84)	(week 24, in vivo) Degradation almost complete, obvious epineurium like tissue observed	Rapid & stable water absorp-tion perfor-mance	(RSC 96 cell line) Proliferation on PLLA/gel higher than PLLA
C. Zheng et al (2021)[29]	(10 mm L) P(LLA-TMC)[r]/ PLLA[a]-0.25% pDNM gel	P(LLA-TMC): 0.65 mm needle; 15 kV; 0.5 mL/h; stain-less steel rod (2 mm Φ); PLLA/0.25% pDNM gel: 20G needle; 15 kV; 1 mL/h; 3000 rpm; 100-mm distance; 20 min; lyophilized	Diam.: ~650 nm (outer), 30–50 nm (inner); Protection tubes (outer) possessed much denser fibers	–	–	–	–	–	–	(DRGs from rats) Highly oriented neurite outgrowth; longer & thicker neurites; large no. of SCs migrating further
Nerve Conduit with Cellular Factors										
Kaka G. et al (2017)[30]	PLGA[r] (10:90)	0.4 mm needle; 20 kV; 1 mL/h	Φ: 100–270 nm	–	–	–	–	–	–	(BMSCs) Seeded BMSCs had more flattened morphology with multiple poses
F. Hu et al (2017)[31]	PHBV-PEO[a] (9:1)	6# needle (0.5 mm Φ); 12 kV; 2500 rpm; 0.5 mL/h	Ave. Φ: 635 nm	–	–	–	–	–	–	(ASCs) Cells grew into 3D scaffolds; confirmed neuronal differentiation of stem cells
S. Das et al (2017)[32]	(1.3 mm Φ, 0.5 mm thickness) Polyaniline-silk fibroin (PASF)[r] (1:100)	15 min distance; 20–25 kV; 0.5–1 mL/h	Ave. Φ: 350–450 nm; Coated with numerous nanosized particles with 40–60nm ave. Φ	–	Resistance: 1×10^{12} Ω	–	11.2 ± 0.3	Swelling ratio (%): 15.3% after 24 h	–	(Rat Schwann cell line, SCTM41) High cellular viability (80%)
S. Farzamfar et al (2018)[33]	(14 mm L, 1 mm Φ) PCL-gelatin[r] (70:30)	18-G needle; 15 cm distance; 20 kV; 0.5 mL/h	Φ: 856 ± 69 nm	Tensile strength: 2.83 ± 0.44 MPa	–	–	76.7 ± 3.2	Weight loss (%): 47.16 ± 3.97 (30th day), 72.46 ± 2.57 (60th day)	66.4 ± 8.1°	(SCs from rats) Showed good attachment and proliferation of cells

(*Continued*)

https://doi.org/10.2147/IJN.S362144

https://doi.org/10.2147/IJN.S362144 DovePress

Table 1 (Continued).

Ref.	Scaffold Materials and Alignment (Shell/Core)	Electrospinning Parameters	Characterization							
			Fiber Diameter	Mechanical Properties	Conductivity	Pore Size (μm)	Porosity (%)	Degradation / Swelling	Surface Hydro-Philicity (WCA)	(In vitro Cell Line) Biocompatibility
F. Pereira dos Santos et al (2019)[33]	(80 μm thickness) PLGA^{r} (75:25)	22 kV; 22G1 needle; 0.002 mL/h	Ave. Φ: 750.3 ± 253.3 nm	–	–	–	–	–	–	(MSCs) Cells keep attached, viable & presented proliferation over time
T. Ma et al (2020)[34]	PCL^{r}/ chitosan (1:6)-PFTBA^{r}	Coaxial: 1.2 mm outer, 0.3 mm inner Φ; core 0.06–0.15 mL/h, shell 0.6 mL/h; 16 kV; 15 cm distance; steel bar (1.5 mm Φ, 180 rpm)	(0.5 mm thickness, 19 mm L, 1.5 mm inner Φ, 2.5 mm outer Φ) Fiber outer Φ: 7.54 ± 2.15 μm, inner Φ: 3.16 ± 2.43 μm	–	–	–	–	–	–	(SCs from rats) Higher viability, less apoptotic cells
Nerve Conduit with Non-Cellular Factors										
Suzuki et al (2017)[36]	PCL^{r}	24G needle; 20 kV; 1.0 mL/h	–	–	–	–	–	–	–	(Cortical neurons from rats) Local administration of MeCbl is effective in promoting axonal outgrowth
Chang et al (2017)[37]	Gelatin-PEO^{a}	25G needle; 18 kV; 0.9 mL/h; 7 cm distance	Φ (nm): 256 ± 12.3 (1500 rpm), 235.7 ± 10.2 (2000 rpm)	Degree of cross-linking increase, with mTG (10~100 U/g-gel), Tensile trength (7.68 ± 0.87~68.96 ± 5.17 kPa) & Young's modulus (57.8 ± 2.63~240.69 ± 6.29 kPa) increase	–	–	–	–	–	(dNSCs; SCs from rats) Long neurite length, cells proliferated and attached well on scaffold
M. Naseri-Nosar et al (2017)[38]	(14 mm L, 1 mm Φ) CA^{r}/PLA^{r}	18 & 24G needles; 18 kV; 1 mL/h; 10 cm distance	Ave. Φ (nm): 834.50 ± 539.66 (uncoated), 945.00 ± 479.97 (coated)	–	–	–	60	(weight-loss % after 40 days) 13.39 ± 0.06 (uncoated), 40.04 ± 4.53 (S+ GNs), 45.02 ± 3.68 (S+ CGNs)	124.55 ± 2.99° (uncoated), 0° (coated)	(SCs from rats) Cells had favorable interaction, more densely packed, elongated & flattened with coated scaffold
Hong et al (2018)[39]	(10 x 15 mm^{2}) 1st layer: PCL^{a} 2nd: PLGA 6535^{r} 3rd: PLGA 8515^{r}	1st: 23G needle, 8.0 kV, 0.5 m/h, 80 mm distance; 2nd & 3rd: 23G needle, 11 kV, 0.5 mL/h, 10 cm distance	–	–	–	Ave.: 34.06	52.48;	–	–	(mNSCs) Cells remained viable & able to proliferate

S. Farzamfar et al (2018)[40]	(14 mm L, 1 mm Φ) CA-gelatin[r]	20G needle; 20 kV; 0.40 mL/h; 15 cm distance	Ave. Φ: 1.78 ± 0.89 μm (scaffold containing GBP 6%)	Ave. ultimate tensile strength: 2.80 ± 0.01 MPa	–	–	69.83 ± 1.61	–	63.67 ± 3.32°	(SCs from rats) Effect of GBP on SCs was dose-dependent; highest viability on CA/gel/GBP 6%
B. Xia et al (2018)[41]	PLLA[r]	16 kV; 0.8 mL/h; 12 cm distance	Φ (μm): 0.68	Young's modulus (MPa): 41.2 ± 14.96; (fresh human nerve: 40.96 ± 2.59)	–	–	–	–	24.3 ± 1.87°	(iPSCs-NCSCs) More than 95% of cells survived
H. Cheong et al (2019)[42]	(15 mm L, 1.2 mm Φ, 900 μm thickness) 10% PLGA[a] (75:25)-10% MAP	11 kV; 0.5 mL/h; 2000 rpm	Size of nanofibers: 20~30 nm	Max. load on repeated external stresses (mM): 0.69 (PLGA/MAP & /MAP-i), 0.8 (PLGA)	–	–	–	–	–	(PC12 cells) PLGA/MAP-I induced the largest cell aspect ratio
J. Sayanagi et al (2019)[43]	PCL sheet[r] /PGA-collagen sponge (PGA-c)	20 kV	–	–	–	–	–	–	–	–
F. Rao et al (2020)[44]	Chitosan-PEO hydrogel[a]	4 kV; 3 mL/h; 60 rpm	Showed aligned orientation of chitosan hydrogel fibers	Elastic modulus: 3.10 ± 0.81 kPa; Tensile strength: 70.66 ± 22.05 kPa; Stress–strain: 39.46 ± 7.20%	–	–	–	–	–	(SCs from rats) ACG regulated the directional growth of SCs
X. Chen et al (2020)[45]	(15 mm L, 2.6 mm Φ, 0.8 mm thickness) PCL[r]	21G needle; 12 kV; 1.5 mL/h	Ave. Φ (nm): 165 (PCL), 117 (composite); Microbeads Φ: 3.8 ± 0.5 μm	Young's modulus (kPa): 622.17 ± 51.58 (PCL), 2490.07 ± 172.15 (SL-M), 2572.89 ± 406.58 (ML-M) Prolongation rate (%): 69.40 ± 6.98 (PCL), 76.41 ± 4.82 (SL-M), 75.58 ± 3.96 (ML-M); Tensile strength (N/mm^2): 0.37 ± 0.04 (PCL), 0.91 ± 0.07 (SL-M), 0.96 ±0.11 (ML-M)	–	–	–	–	–	(RSC 96 cell line) Composite scaffolds had higher cell viability (~90%) and more proliferative cells

(*Continued*)

https://doi.org/10.2147/IJN.S362144

Table 1 (Continued).

Ref.	Scaffold Materials and Alignment (Shell/Core)	Electrospinning Parameters	Characterization							
			Fiber Diameter	Mechanical Properties	Conductivity	Pore Size (μm)	Porosity (%)	Degradation / Swelling	Surface Hydro-Philicity (WCA)	(In vitro Cell Line) Biocompatibility
S. Amini et al (2020)[46]	(12 mm L, 1.6 mm inner Φ, 2 mm outer Φ, 0.4 mm thickness) PCL[a]	21G needle; 19 kV; 20.0 cm; 0.5 mL/h; 2000 rpm	Mean Φ (nm): 334 ± 86 (P10L), 364 ± 97 (P15L)	Young's modulus (MPa): 1.2 ± 0.3 (P10L), 0.303 ± 0.1 (P15L); UTS (MPa): 7.4 ± 1.4 (P10L), 2.15 ± 0.7 (P15L); Elongation at break (%): 14 ± 3 (P10L), 12 ± 2 (P15L)	–	–	–	Water uptake value (%): 257 ± 27 (P10L), 292 ± 32 (P15L); Weight loss (%): (after 1 mth) 8.4 ± 1.3 (P10L), 10.2 ± 1.4 (P15L); (2 mths) 16.1 ± 1.5 (P10L), 18.2 ± 1.6 (P15L)	25.31 ± 6° (P10L), 41.88 ± 8° (P15L)	(hADSCs) High cell viability; Elongated neurite outgrowth; Cells are positive for MSC marker and negative for hematopoietic stem cell marker
H. Samadian et al (2020)[47]	PCL-gelatin[r] (30:70)	20 kV; 0.5 mL/h; 15 cm distance	Φ: 708 ± 476 nm	Tensile strength: 5.31 ± 0.97 MPa; Young's modulus: 3.47 ± 0.10 GPa	–	–	51.27 ± 6.27	(weight loss %) 27.33 ± 1.90 (30 days), 41.60 ± 6.94 (60 days)	78.30 ± 2.52°	(SCs from rats) Nanofibers are biocompatible & non-toxic
Nerve Conduit with Combination Strategy (Cellular + Non-Cellular Factors)										
H.K. Jahromi et al (2020)[48]	PLLA-surface-modified multi-wall carbon nanotubes (0.25 wt% mMWCNT)[r]	22G needle; 18 kV; 1 mL/h; 1 mm Φ mandrel; 100 rpm; 9 cm distance	Wall thickness: 300–325 μm; Φ (mm): 3.1 ± 0.3 (inner), 3.3 ± 1.2 (outer); Fiber Φ: 2.3 ± 0.7 μm	Tensile strength (MPa): 3 (day 0), 2.5 (day 60)	–	–	89 ± 3	Swelling (%): 135 (12 h), 150 (24 h), 160 (48 h), 155 (120 h); Degradation (mass loss %): 10 (7 d), 15 (14 d), 25 (28 d), 58 (60 d)	79.3 ± 1.8°	(SCs from rats) High viability of cells; Cells attach & grow on the surface by normal spindle shape
G. Zhou et al (2020)[49]	(17 mm L, 60 μm thickness) PCL[a]	5.5 cm distance; 10.5 kV; 0.25 mL/h	Random outer surface, aligned inner surface; Gap between each layer: 100–150 μm	–	–	–	–	–	–	(PC12 cells) Longest mean lengths of PC12 neurite extension on scaffold
M. Jahromi et al (2021)[50]	(2 mm Φ) Laminin-coated PLGA[a] (80:20)	27G needle; 21 kV; 250 μL/h; 15 cm distance	Ave. thickness: 73.8 ± 2.05 μm; Mean thickness of laminin-coated PLGA + filler: 77.8 ± 2.05 μm	–	–	–	–	–	–	–

Abbreviations: a, aligned electrospun fiber; r, random electrospun fiber; f, freeze-dried polymer; CNF, carbon nanofiber; pDNM, decellularized matrix hydrogel derived from porcine sciatic nerves; CA, cellulose acetate.

studies include PC12 cells, SCs, DRG cell lines, RSC96 cell line, A-172 cell line, bone marrow stromal cells (BMSCs), adipose-derived stem cells (ASCs), SCTM41 cell line, cortical neurons, neural stem cells (NSCs) and induced pluripotent stem cells–neural crest stem cells (iPSCs-NCSCs). Furthermore, biocompatibility tests provide researchers to observe the tolerability of cells and whether the scaffolds are suitable for in vivo implantation.

Additional Factors

Apart from providing topological support for facilitating nerve regeneration, researchers believe that the additional chemical or biological factors, such as neurotrophic factors, drugs, bio-functional peptides or cells-seeded on conduit, can boost the regeneration further (Tables 2 and 3). Most of the studies used single factors, such as cells only or drugs only; whilst 3 studies[48–50] used combination strategies, combining cells and neurotrophic factors or drugs.

Cells

Cell therapy acts as a nerve repair strategy which creates a favorable environment in the peripheral nervous system.[60] Mesenchymal stem cells (MSCs) are the most popular candidate for providing biological support for nerve regeneration (Table 2). The sources of MSCs were mostly bone marrow cavity (BMSCs),[30,49] adipose tissue (ADSCs, ASCs)[31,48] and exfoliated deciduous teeth pulp (SHED).[34] Researchers have demonstrated that MSCs can replace lost neurons and non-neuronal cells by differentiating them into the neural lineage or by providing trophic support for the repair process.[59] Thus MSCs, with their ease of accessibility, fast proliferation rate, differentiation potential and inherent ability to secret nerve growth factor,[61] are a suitable cell source for the cell-based treatment of peripheral nerve injury. Neural differentiation is better to be performed during cell culture to ensure that the stem cells will grow into neural lineage, whereas only Hu et al[31] have clearly stated that they have performed neural differentiation. Furthermore, recent studies have indicated that as a gene manipulation strategy, the regulation of microRNA (miRNA) expression levels has been useful for facilitating stem cell neuronal differentiation and neurogenesis, with profound value for nerve regeneration.[62] Hu et al[31] have identified an original approach to stem cell transformation based on temporally sequential treatment with Fibroblast Growth Factor 2 (FGF2) and miR-218 to promote ASCs neuronal differentiation.[63]

SCs are essential for nerve regeneration, as they are responsible to form myelin in the peripheral nervous system, secrete neurotrophins and produce extracellular matrix molecules to facilitate axonal outgrowth and elongation.[64] MSCs are believed to be differentiated to SC-like cells, however, this could be complicated and unstable. As a result, several groups of researchers[32,35,48] tend to seed SCs directly onto the conduit, rather than attempting to turn stem cells into SCs. As shown in Table 2, the cell source of SCs is mainly from sciatic nerves.

Sources for cells were mainly from rats, as the nerve graft would be implanted to a rat nerve defect model. Only Farzamfar et al[40] and Pereira dos Santos et al[34] used stem cells from human instead of rats, without applying any immunosuppressant, which may bring immunological rejected concerns to the studies. Nevertheless, 3rd–5th passage of cells had been used, and cell numbers varied from 1.42×10^4 to 2×10^6 cells in each conduit. Moreover, cell fate tracking is important as researchers should have a better and clearer understanding about the condition of their seeded cells on the conduit after in vivo implantation. It is important to know whether the seeded cells have successfully been turned into neural lineage, or they provide environmental support without turning into SCs. Disappointedly, only Ma et al[35] have engineered the seeded cells for cell fate tracking.

Although incomplete, they manage to demonstrate how their seeded SCs interacted with their fabricated nerve conduit, after 14 days of surgery. They used fluorescence protein for tracking the seeded SCs, to measure the viability of SCs after implantation, and they found that SCs seeded on PFTBA fabricated nerve conduit produced the highest viability of SCs while comparing to only PCL fabricated nerve conduits.

The best strategy for nerve regeneration should be supported by the results of in vivo implantation in an animal nerve defect model, which will be discussed later.

Neurotrophic Factors (NFs)

NFs that have been used for nerve regeneration include brain-derived neurotrophic factor (BDNF),[37,39,50], nerve growth factor (NGF),[37,41,49] neurotrophin-3 (NT-3),[39] platelet-derived growth factor (PDGF)[39], vascular endothelial growth

Table 2 Comparison of the Sources of Cells Seeded on Nerve Conduits and Their Manipulations

Papers	Cell Type	Cell Source	Media	Passage Number	Number of Cells (Density)	Characterization	Manipulation
Kaka et al (2017)[30]	Bone marrow stromal cells (BMSCs)	From femurs of 3 Wistar rats	α-MEM suppl. with 10% FBS, 1% P/S	3rd passage	–	–	–
Hu et al (2017)[31]	Adipose-derived mesenchymal stem cells (ASCs)	Adipose tissue from SD rats;	Basal medium: DMEM, 5% FBS, 1% P/S, 10 ng/mL fibroblast growth factor 2 (FGF2)	–	6×10^4 cells in each conduit	βIII-Tubulin expression confirmed the neuronal differentiation of stem cells	Neuronal differentiation: basal medium suppl. with 100 ng/mL Retinoic Acid; transfected with miR-218 Plasmid
Das et al (2017)[32]	Rat Schwann cell line (SCTM41)	Post-natal sciatic nerve cultures of SD rats;	DMEM containing 10% FBS	–	1×10^5 cells in each conduit	–	–
Farzamfar et al (2018)[33]	Human unrestricted somatic stem cells (hUSSC)	Umbilical cord vein blood	Low-glucose DMEM suppl. with 30% FCS, 10^{-7} M dexamethasone, 100 unit/mL penicillin, 100 μg/mL streptomycin, 2 mM ultraglutamine	–	3×10^4 cells in each conduit	Demonstrated fibroblast-like morphology; Positive for CD73, CD105, CD166, negative for CD34, CD45	–
Pereira dos Santos et al (2019)[34]	Mesenchymal stem cells (MSCs)	Human exfoliated deciduous teeth pulp (SHED)	DMEM-low glucose/Hepes, suppl. with 10% FBS, 100 unit/mL penicillin, 100 μg/mL streptomycin, 0.45 μg/mL gentamicin	5th passage	1.42×10^4 cells in each conduit	MSC expressed negatively to CD14 (1.2%), CD34 (0%), CD45 (0.6%), CD184 (0.7%), HLA-Dr (0.4%), STRO-1 (0.5%), positively to CD29 (96.8%), CD90 (98.6%), CD73 (98.4%)	–
Ma et al (2020)[35]	SCs in fibrin gel (SCs/gel)	Sciatic nerves from 2-day-old SD rats	FBS, mitogen medium (20 mg/mL bovine pituitary extract), 4 mM forskolin, 10 ng/mL bFGF	3rd passage	1×10^6 cells in each conduit	Annexin V-FITC/PI staining and flow cytometry analysis confirmed growth of cells; immunostained with S100 confirmed cell adhesion	SCs were engineered to express GFP through retrovirus-mediated delivery
Jahromi et al (2020)[48]	Primary SCs	Sciatic nerves of healthy male Wistar rats (4 months old, 240–280 g)	DMEM/F12 suppl. with 1% P/S, 1% amphotericin, 10% FBS	3rd passage	1×10^6 cells in each conduit (suspended in the prepared fibrinogen solution)	(P75, S100, DAPI staining) Bipolar spindle shape; P75 expression: 60.94 ± 6.06%; S100 expression: 92.84 ± 4.57%	–
Zhou et al (2020)[49]	Bone marrow stromal cells (BMSCs)	Bone marrow cavity of adult male SD rat (250–300 g)	α-MEM suppl. with 10% FBS, 1% penicillin, cultured in rotary cell culture system (RCCS)	3rd passage	2×10^6 cells in each conduit	Post-surgical cell viability assessments: GFP-SCs Highest no. of SCs on PFTBA conduit	–
Jahromi et al (2021)[50]	r-ADSCs	Subcutaneous adipose tissue in inguinal region of adult male Wistar rats	DMEM + 10% FBS; suspended in alginate	3rd–4th passage	2×10^6 cells in each conduit	Microscope image: r-ADSCs had fibroblast-like form, appeared regular, and were larger in size	–

factor (VEGF)[41] and platelet-rich plasma (PRP).[47] These NFs were carried by gelatin nanoparticles or solution, hydrogel, chitosan nanoparticles, as well as directly incorporated onto the electrospun fibers with different release profile (sustained, gradual or accumulated release), as shown in Table 3.

BDNF is important in NSCs proliferation, differentiation and directional migration.[65] Adding exogenous BDNF enhances myelination, whereas the removal of endogenous BDNF inhibits the formation of mature myelin internodes.[66]

NGF plays a vital role in nerve cell growth, differentiation, regeneration and neurotransmitter homeostasis,[67] and prevents neuronal degeneration in animal models with encouraging results.[68] NGF has been widely employed to maintain

Table 3 Comparison of Non-Cellular Factors (Growth Factors, Drugs, Peptides) Added to the Nerve Conduits

Paper	Additional Factors	Carriers	Characterization	Drug/Neurotrophic Factor Release Profile
Suzuki et al (2017)[36]	MeCbl	Incorporated with fibers	–	Chemiluminescence immunoassay – Sustained release: 14.6 ± 0.9% (1%), 9.8 ± 0.7% (2%), 12.1 ± 1.4 (3%)
Chang et al (2017)[37]	BDNF (BDNF-GN); Neurotrophic gradient of NGF from 6.6~107.2 ng/mL	Gelatin nanoparticles; Gelatin solution	BDNF-GN particle size: 262.70 ± 78.46 nm; Drug loading: 35.31 ± 0.63%; Encapsulation efficiency: 70.61 ± 1.26%	ELISA – Gradual release of BDNF (slowly diffused out from GN), rapid release of NGF (which dispersed within the gel scaffold)
Naseri Nosar et al (2017)[38]	Citalopram hydrobromide (CGNs)	Gelatin nanocarriers	SEM: ave. Φ of CGNs: 539.50 ± 277.95 nm	–
Hong et al (2018)[39]	BDNF, NT-3 & PDGF	Hydrogel micro-patterning ("stapler")	SEM – overall thickness: 140 μm – PCL: 30 μm; PLGA 6535 & 8515: 55–60 μm	ELISA – NT-3 & BDNF released faster than PDGF, as PLGA 6535 with lower lactide/glycolide ratio which degraded faster – Showed sustained release: release profile form PLGA 6535 & PLGA 8515 reached plateau after 6 & 8 weeks respectively
Farzamfar et al (2018)[40]	Gabapentin (GBP)	Water/ethanol (3:7) coagulated	–	–
Xia et al (2018)[41]	NGF, VEGF	Incorporated with fibers	FITC-labeled NGF solution, TEM – Inner dark core: water phase contained NGF – Bright outer shell: oil phase composed of PLLA	ELISA, accumulated release % of drug – VEGF: 35.72 ± 0.29 (within 1 day), 58.56 ± 1.31 (4th day); – NGF: 4.86 ± 1.00 (within 1 day), 15.01 ± 0.12 (initial 3 days), 29.52 ± 0.91 (11th day)
Cheong et al (2019)[42]	ECM-derived biofunctional peptides (IKVAV) (MAP-i)	Incorporated with fibers	SDS-PAGE – MAP and its fusion variants were all successfully produced in bacterial system with high purities over 90%	–
Sayanagi et al (2019)[43]	3% MeCbl	Incorporated with fibers	–	Chemiluminescence immunoassay – Stable sustained MeCbl release for up to 38 weeks, 30.2 ± 0.4%
Rao et al (2020)[44]	Functional polypeptides RGI & KLT	Hydrogel	HPLC: > 95% purity	–
Chen et al (2020)[45]	1% Fe3O4-magnetic nanoparticles (MNPs), 1% melatonin (MLT)	Incorporated with fibers	–	HPLC – Almost 80% of MLT release from multi-layered scaffold within 7 d, from single-layer scaffold was only 54% even after 21 d
Amini et al (2020)[46]	Kraft 10% & 15% lignin (P10L, P15L)	Nanoparticles incorporated with fibers	Ave. particle size: ~ 90 nm	–
Samadian et al (2020)[47]	Platelet-rich plasma (PRP) fr. blood of rats; 100 μmol/h Citicoline	PRP gel (isolated PRP + 10 wt% $CaCl_2$ + 300 IU thrombin)	–	UV-visible spectroscopy – Exhibited sustained release & approximately 50% of citicoline released during 14 days Hemolysis %, hemocompatibility – red blood cells lysis: PCL/gel nanofibers induced some degree of hemolysis; incorporation of PRP & citicoline increased the hemocompatibility
Jahromi et al (2020)[48]	Curcumin (nanocurcumin, NC)	Chitosan nanoparticles	Encapsulation efficiency (EE) – concentration of curcumin increase, EE increase; Dynamic light scattering (DLS) & SEM – particle size distribution (μm): 0.1–1.5, concentrated at 0.6 FTIR-ATR – confirm successful encapsulation of curcumin inside chitosan MPs	~70% DOX release at the first 144 h (sustained release)
Zhou et al (2020)[49]	NGF	Incorporated with fibers	–	–
Jahromi et al (2021)[50]	AuNPs & BDNF (AuNPs- or BDNF-CNPs)	Chitosan nanoparticles	–	(after 7 days) BDNF: 74 ± 2.42% AuNPs: 47.24 ± 1.78%

neuronal differentiation and promote the proliferation of pheochromocytoma cells.[69] Moreover, the axonal growth of the neural cells was significantly enhanced in a dose-dependent manner of NGF.[70]

NT-3 is known to proliferate fibroblasts to help the nerve regeneration in a rat model.[71] NT-3 usually works in combination with BDNF to promote axonal regeneration and behavioural outcomes.[72] The combined secretion of NT-3 and BDNF usually occurs in vivo for cellular proliferation before the differentiation stage.[73]

PDGF acts as a mitogen and protects against neuronal degeneration, which induces the neurogenesis in the post-mitotic stage, where the differentiation stage would start to dominate the proliferative states.[74] With a sustained release manner from conduit, the later appearance of PDGF would further extend the neurogenesis process,[75] which creates a better environment for the nerve regeneration process.

VEGF is capable of increasing vascular permeability, endothelial cell proliferation, migration, survival and angiogenesis.[76] It has been shown to stimulate SCs invasion and neovascularization.[77]

PRP, the platelet-enriched compartment of centrifuged whole blood, contains a high concentration of various proteins and growth factors (GFs) such as PDGF, VEGF, transforming growth factor (TGF-β1), epidermal growth factor (EGF), insulin-like growth factor (IGF) and basic fibroblast growth factor (bFGF).[78] Due to its abundant contents, it is usually used as a complementary treatment for periodontal tissue disease, dental implants, burns, dermatology, musculoskeletal system disruption, as well as nerve regeneration.[79]

Bio-Functional Peptides

The ability of MAP to confer cell adhesion, cell proliferation and tissue regeneration is due to its unique adhesive property and biocompatibility, thus making it an alternative to conventional synthetic polymer-based nerve conduits.[80] Interestingly, it is capable of the genetic incorporation of various bio-functional peptides,[81] such as the bio-functional peptide that derived from ECM, which is IKVAV. The bio-functional peptide plays crucial roles in tissue regeneration through diverse integrin-mediated pathways.[82] Cheong et al[42] found that incorporating bio-functional peptide into a material, especially MAP, can intrinsically enhance its regenerative capacity, which maintains the effectiveness of a peptide for prolonged period.

Apart from that, short peptide fragments with cell-specific functions can mimic the functions of growth factors and significantly improve the biological function and specificity of materials. Bioactive RGI peptide derived from BDNF plays an important role in motor neuron outgrowth.[83] Peptide KLT simulates the functional segment of VEGF which as stated earlier is important in angiogenesis. Peptide KLT acts as an analog and is the only synthetic peptide that can activate the VEGF receptor.[84] A combination of KLT and RGI can potentially promote microcirculation reconstruction and recovery of motor function.[44]

Drugs

Drugs that have been used by studies include methylcobalamin (MeCbl),[36,43] citalopram hydrobromide (CTL),[38] gabapentin (GBP),[40] melatonin (MLT),[45] lignin,[46] citicoline (CTC)[47] and curcumin.[48] These drugs were carried by gelatin nanocarriers or particles, chitosan nanoparticles, as well as water/ethanol (3:7) coagulated or directly incorporated with the electrospun fibers, and result in different release profiles (sustained, gradual or accumulated release), as shown in Table 3.

MeCbl is one of the active forms of vitamin B12 homologues. It is delivered favorably to nerve tissues and effective in promoting nerve regeneration and neuronal cell survival.[85] It promotes neurite outgrowth and neuronal survival in cerebellar granule neurons and DRG neurons, which improves functional and electrophysiological results in a rat sciatic nerve transection model.[86] High concentrations of MeCbl are likely to be necessary to maximize effectiveness in promoting nerve regeneration.

CTL is a blood–brain barrier permeable bioactive molecule, selective serotonin reuptake inhibitor antidepressant, as well as a widely used drug for many mental disorders such as depression and anxiety.[87] It promotes neuronal cell proliferation and enhances neuroplasticity.[88]

GBP is an anticonvulsant drug used as an analgesic to control neuropathic pain.[89] It is able to enhance the nerve remyelination after chronic constriction of the sciatic nerve, suggesting its application for nerve regeneration.[90]

MLT is an indoleamine that has neuroprotective and anti-inflammatory effects that protects cells from reactive oxygen species and reactive nitrogen species.[91] It is effective in scavenging free radicals, inhibiting apoptosis, preventing scar formation and cytoskeletal remodeling.[92] It might be an anti-inflammatory agent as it can regulate expression of proinflammatory cytokines and transcription factors related to antioxidant response such as NFκB and Nrf2.[93] Thus, loading MLT on nerve conduit may help to reduce the inflammatory response after surgery.

Lignin has antioxidant, antimicrobial and stabilizer properties. Therefore, it can act as a scavenger of oxygen free radical for sustaining the reactions initiated by oxygen radicals, and at the same time promotes neural cell viability, proliferation and differentiation.[94]

Phosphatidylcholine is the primary component of neuron membrane, while CTC is a choline donating intermediate in the biosynthesis of phosphatidylcholine. As a result, CTC is beneficial for cognitive impairment of diverse etiology, treatment of cerebrovascular disease, Parkinson's disease (PD) and head trauma,[95] which exhibited neuroprotective activities. Intraperitoneal and topical administration of CTC may enhance the anatomical regeneration and functional recovery of PNI.[96]

Curcumin has a great potential ability in the regeneration of injured peripheral nervous system (PNS)[97] and protect dorsal root ganglion.[98] It is effective in the proliferation and differentiation of SCs,[99] which significantly decrease the apoptosis of SCs and dramatically increase the number of myelinated axons in the injured sciatic nerve.[100]

Others

Chen et al[45] adopted Iron (II, III) oxide-magnetic nanoparticles (Fe_3O_4-MNPs) as an additional factor to nerve conduit. Fe_3O_4, with certain superparamagnetic properties, is capable of inducing axonal extension or direct neurite outgrowth under an external magnetic field without any side effects.[101] Fe_3O_4 nanoparticles can also enhance neurite outgrowth by activating the mitogen activated protein kinase signaling pathway.[102]

Jahromi et al[50] employed gold nanoparticles (AuNPs) which may enhance the cell–material interactions in terms of cell adhesion, proliferation, differentiation, stimulate axonal elongation and sprouting axons.[103]

By all possible means, the best strategy for nerve regeneration should be supported by the results of in vivo implantation in an animal nerve defect model, which will be discussed later.

Preclinical Model

An animal defect model is the most important part for in vivo investigation. The size and species of the animals may reflect the level of studies, as studies from rats, rabbits, monkeys or humans are hugely different. Almost all of the studies adopted Lewis rats, SD rats or Wistar rats. Only 1 out of 39 studies[37] adopted New Zealand white rabbits for in vivo nerve regeneration study. With respect to the anatomical site of the investigation, 38 employed sciatic nerve defect, and only 1 employed median nerve[21]. The defect size and duration of implantation were at the range of 7–15 mm and 4–48 weeks, respectively (Table 4).

Although almost all of the studies created a segmental nerve defect. One study crushed the nerve from sciatic notch[36] and another clamped the sciatic nerve by micro clamp[39]. For both of these studies, researchers utilized tools to dysfunction the nerve, then wrapped the electrospun fiber sheet around the injured site, to serve as a nerve "conduit".

Outcomes

Functional Assessments

The functional outcomes, brief information and data of those 39 in vivo peripheral nerve repair studies are listed in Table 4. Statistically, $p < 0.05$ and N.S. indicate significant difference and not significant respectively, and are important and symbolic to a randomized study. However, some studies[22,32,49] discussed their results without providing enough statistical comparison. Thus, in this review, only those quantitative results with statistical analysis will be focused and discussed in detail.

Studies will be compared within groups, whereby the groups will be divided according to the duration of their study. In summary: 2 studies in the group of 60 days, 6 studies in the group of 8 weeks, 18 studies in the group of 12 weeks, and 2 studies in the group of 14 weeks, total 4 groups to be compared; those 12 studies which are not belonging to these 4

groups are not comparable as their animal model or duration of implantation are unique and different with others, thus they were listed as a reference. Besides, the experimental groups within a study have been standardized as: autograft group (A), normal group (sham operation, without surgery; P), negative control group (injured nerve without treatment; N) and other treatment groups (B and C). The details of each group are labeled in Table 4.

During the functional assessments or examinations, researchers should always compare the defect site to the normal site of the model. There are some terms that are common in functional assessment of an animal nerve defect model: sciatic functional index (SFI) for motor functional analysis; hot plate latency (HPL) and paw withdrawal latency (PWL) for sensory recovery analysis; muscle weight measurement for muscle atrophy analysis after surgery; Masson Trichrome (MT) staining for muscle and collagen fiber staining; and amplitude of compound muscle action potential (CMAP), nerve conduction velocity (NCV) and time latency of compound muscle action potential (TL) that belong to the electrophysiological examination, which correspond to the area and size of axons and level of myelination.

For the 2 studies in the group of 60 days, they are not comparable as Naseri-Nosar et al[38] did not compare their experimental groups with the autograft group while Farzamfar et al[40] did. Interestingly, it seems like GBP truly provided its beneficial effect on enhancing remyelination and hence promoted the nerve regeneration as Farzamfar et al[40] showed us the great performance of the experimental group which have no significant difference to the autograft group only after 60 days of implantation. Although there was no autograft group to be compared in the study by Naseri-Nosar et al[38], their result stated that the functional recovery of experimental group with CTL was significantly better than without CTL.

Within the group of 8 weeks, only Zhang et al[17] who adopted aligned PHBV/PEO fibers, showed significantly greater SFI in the nanofibers group compared to the autograft group. However, they only evaluated SFI, thus, it should not be overgeneralized to say that their strategy is better. Nonetheless, both Song et al[13] and Moharrami Kasmaie et al[27] who adopted aligned PPY/PLCL and PCL/PLGA fibers, respectively, have shown that no significant difference between experimental groups and autograft group. However, Kaka et al[30], and Cheong et al[42] and Zheng et al[29] have shown inferior results in the experimental group, even with the addition of BMSCs or bio-functional peptides. This may due a short duration of 8 weeks which may not be enough for effective functional recovery.

Within the group of 12 weeks, Zhang et al[14], Sun et al[19], Ma et al[35] and Jahromi et al[48] have shown no significant difference between experimental groups and the autograft group. As expected, Ma et al[35] who adopted oxygen releasing PFTBA fibers with seeded-SCs, and Jahromi et al[48] who employed the combination strategy of aligned fibrin fibers with SCs and curcumin, have shown better results than the other 16 studies in the group of 12 weeks. Jahromi et al[50] using the combination strategy of aligned PLGA fibers with r-ADSCs, AuNPs, BDNF and alginate showed significant difference between experimental groups, in which the group with all additional factors "seeded" on the conduit was significantly better than the group with PLGA fibers only. However, they did not compare their experimental groups with the autograft group.

For the 2 studies in the group of 14 weeks, they are not comparable as Lopez et al[21] did not compare their experimental groups with the autograft group while Farzamfar et al[40] did. However, it could be said that these 2 studies did not have satisfying results. Lopez et al[21] failed to show better performance of nanowrap compared to autograft. Farzamfar et al[40] adopted human unrestricted somatic stem cells (hUSSCs) from umbilical cord to be seeded on nerve conduit. The result of the autograft group was still significantly better than the experimental group, especially the value of SFI and muscle weight loss percentage. This is probably due to the immunosuppressive effect as they employed stem cells from human source without applying any immunosuppressant. However, we should correspond the functional and histological results together to give a better conclusion, which will be discussed in a later part.

It is known that animals may have tendency to self-harm (autotomy) due to the neuropathic pain and inflammations after surgery. Administration of pain-killer or antibiotics may help to alleviate the inflammatory symptoms. However, only 7 out of 39 studies[14,25,27,32,45,46,49] have reported the application of pain-killer or antibiotics after surgery to avoid serious inflammation and other adverse effects. These drugs were administered only for short durations post-operatively and not the entire duration of the study.

Gene and Protein Expression and Morphometric Assessments

As a matter of fact, the more the number of axons, the larger the CAMP; the larger the diameter of axons, the faster the NCV. Thus, there would be a strong relationship between functional and morphometric outcomes.

Table 4 Comparison of Functional Outcomes of Peripheral Nerve Repair of All Studies

Paper	Animal		Functional Assessment									
	Species, Weight, Part of Incision	Experiment Group	Administration of Pain-Killer/ Antibiotics	Motor Function Analysis		Muscle Weight	Masson Trichrome Staining	Electrophysiological Examination			Sensory Recovery (HPL / PWL)	Duration
				SFI	Other			CMAP (mV)	NCV (m/s)	TL (ms)		
Nerve Conduit with Micro- or Nano-Fiber Only												
Zhou et al (2016)[12]	Male SD rats, 200–250 g; Right sciatic nerve (10 mm gap)	A: autograft B: PELA C: PELA-20% PPY	–	($p < 0.05$) –42 (A), –68 (B), –38 (C)	–	(relative weight, %) ($p < 0.05$) 70 (A), 40 (B), 69 (C)	–	($p < 0.05$) 5.8 (A), 2.1 (B), 4.5 (C)	($p < 0.05$) 58 (A), 20 (B), 45 (C)	–	–	12 weeks
Song et al (2016)[13]	30 male SD rats (200–250 g); Right sciatic nerve (15 mm gap)	A: autograft B: PPY/ PLCL + 100 mV ES	–	(N.S.) –21.4 ± 1.1 (A), –23.5 ± 1.2 (B)	–	(N.S.) (relative weight, %) 95 (A), 90 (B)	–	(N.S.) 9.34 ± 0.12 (A), 8.07 ± 0.24 (B)	(N.S.) 63.32 ± 2.54 (A), 61.34 ± 4.21 (B)	–	–	8 weeks
Zhang et al (2016)[14]	30 adult SD rats, 200–250 g; Right sciatic nerve (10 mm gap)	A: autograft B: PLGA-SF-CL	Penicillin (800,000 IU/ kg i.m.) was administered after surgical operation	–	–	–	(N.S.) Muscle fiber diam. (μm): 42.47 ± 0.39 (A), 40.24 ± 0.46 (B)	(N.S.) 4.58 ± 0.11 (A), 4.42 ± 0.12 (B)	(N.S.) 31.02 ± 0.34 (A), 30.82 ± 0.42 (B)	–	–	12 weeks
Du et al (2017)[15]	87 male SD rats, 200–220 g; 7-mm segment of sciatic nerve (10 mm gap)	A: autograft B: aligned-fiber conduit	–	($p < 0.05$) –40 (A), –42 (B)	–	($p < 0.05$) Wet weight ratio: 0.78 (A); 0.58 (B)	($p < 0.05$) Collagen fiber area %: 82 (A); 62 (B)	($p < 0.05$) 10.0 (A); 6.8 (B)	–	($p < 0.05$) 1.70 (A); 1.75 (B)	–	12 weeks
Sun et al (2017)[16]	Male/female AD rats, 200–250 g; Left leg sciatic nerve (10 mm gap)	A: autograft B: NS-containing conduit	–	(N.S.) –40 (A); –42 (B)	–	(N.S.) Relative weight (%) 83 (A); 80 (B)	($p < 0.05$) Collagen fiber area %: 7 (A); 14 (B)	–	–	–	–	12 weeks
Zhang et al (2018)[17]	Adult SD rats, 200–250 g; Right sciatic nerve (12 mm gap)	B: aligned PHBV/PEO C: blank control group	–	($p < 0.05$) –55 (B), –98 (C)	–	–	–	–	–	–	–	8 weeks
Jing et al (2018)[18]	24 young adult male SD rats, 180–220 g; Sciatic nerve (8 mm gap)	A: autograft B: PP-POP	–	($p < 0.05$) –35 (A), –45 (B)	–	–	–	($p < 0.005$) 3.05 ± 0.071 (A), 1.395 ± 0.388 (B)	($p < 0.05$) 40 ± 5.3 (A), 32 ± 4.1 (B)	(N.S.) 0.675 ± 0.021 (A), 0.719 ± 0.027 (B)	–	12 weeks

(*Continued*)

https://doi.org/10.2147/IJN.S362144 DovePress

Table 4 (Continued).

Paper	Animal		Functional Assessment									
	Species, Weight, Part of Incision	Experiment Group	Administration of Pain-Killer/ Antibiotics	Motor Function Analysis		Muscle Weight	Masson Trichrome Staining	Electrophysiological Examination			Sensory Recovery (HPL / PWL)	Duration
				SFI	Other			CMAP (mV)	NCV (m/s)	TL (ms)		
Sun et al (2019)[19]	18 adult male SD rats, 200–250 g; Left sciatic nerves (10 mm gap)	A: autograft B: PPy-PLCL/SF conduit	–	(N.S.) –40 (A), –44 (B)	–	–	–	–	–	–	–	12 weeks
Farzamfar et al (2019)[20]	Male Wistar rats (3 months old), 250–270 g; Right sciatic nerve (10 mm gap)	A: autograft B: PCL/CNF conduit	–	($p < 0.05$) –35.66 ± 3.21 (A), –45.66 ± 3.05 (B)	–	($p < 0.01$) (Weight loss %) 8.42 ± 2.41 (A), 13.66 ± 1.52 (B)	–	($p < 0.05$) 26.45 ± 2.54 (A), 20.66 ± 3.05 (B)	–	–	($p < 0.05$) HPL (s): 5.33 ± 0.76 (A), 7.33 ± 0.57 (B)	12 weeks
Lopez et al (2019)[21]	15 male Lewis rats, 250–300 g; 10 mm median nerve segment	B: without nano-wrap C: with nano-wrap	–	–	($p < 0.05$) Grip strength (N): 0.68 ± 0.22 (B, regained 25.4%), 5.39 ± 0.63 (C, regained 34.9%)	($p < 0.05$) Ave. limb flexor muscles weight (g): 0.511 ± 0.07 (B), 0.629 ± 0.054 (C)	–	($p = 0.182$) 0.460 ± 0.207 (B), 0.941 ± 0.706 (C)	–	($p = 0.194$) 2.820 ± 0.593 (B), 2.425 ± 0.190 (C)	–	14 weeks
Yen et al (2019)[22]	48 adult male SD rats, 250–300 g; Left sciatic nerve (10 mm gap)	B: PCL only C: PCL + type I collagen	–	–82 (B), –58.77 (C)	–	–	–	–	–	–	–	8 weeks
Wang et al (2019)[23]	Male SD rats; 10 mm sciatic nerve defect	A: autograft B: GO-ApF /PLCL	–	–	–	(N.S.) (relative weight, %)90 (A), 80 (B)	($p < 0.05$) Collagen fiber area %: 2.5 (A), 4 (B)	–	(N.S.) 25 (A), 23 (B)	–	–	12 weeks
Neshat et al (2020)[24]	Young adult male SD rats, 150–180 g; Right sciatic nerve (10 mm gap)	B: non-implanted C: P-CA	–	–56.79 ± 2.23 (C)	SSI: –50.60 ± 3.63 (C)	($p < 0.05$) (relative weight, %) 50 (B), 767.7 (C)	–	($p < 0.05$) (Recovery index of EMG, mv/mv) 0.14 ± 0.06 (B), 0.37 ± 0.4 (C)	–	($p < 0.05$) 1.4 ± 0.34 (B), 1.29 ± 0.32 (C)	–	7 weeks
Wang et al (2020)[25]	24 female SD rats, 200–250 g; Right sciatic nerve (10 mm gap)	A: autograft B: multiple aligned (M-A)	Injected with 800,000 units of penicillin immediately after surgery to prevent infection	–	–	–	–	($p < 0.01$) 11.17 ± 1.05 (A), 6.43 ± 0.25 (B)	($p < 0.01$) 55.86 ± 5.08 (A), 45.07 ± 5.39 (B)	–	–	12 weeks

https://doi.org/10.2147/IJN.S362144 DovePress

Zhang et al (2020)[26]	30 adult male SD rats (200–220 g); Right sciatic nerve (10 mm gap)	A: autograft B: HO-PSNC -20	–	(N.S.) –45 (A), –55 (B)	–	(N.S.) (relative weight, %)63 (A), 55 (B)	(N.S.) Muscle fiber area (μm2): 1250 (A), 1150 (B); Collagen Fiber Area %: 10 (A), 12.5 (B)	($p < 0.05$) 18 (A), 14 (B)	($p < 0.05$) 11 (A), 14 (B)	($p < 0.05$) 5 (A), 7 (B)	–	12 weeks
Moharrami Kasmaie et al (2021)[27]	32 young adult male Wistar rats (250 & 300 g); Left sciatic nerve (7 mm gap)	A: autograft B: PCL/ PLGA	Injected with Carprofen 5 (mg/kg) subcutaneously for 3 days to minimize the pain	(N.S.) –43.1 ± 12.42 (A), –47.6 ± 5.06 (B)	–	(N.S.) (relative weight, %) 47.88 ± 13.53 (A), 38.08 ± 11.76 (B)	–	(N.S.) 1.4 ± 0.14 (A), 1.78 ± 0.5 (B)	–	–	–	8 weeks
Niu et al (2021)[28]	Male SD rats, 250–350 g; Right sciatic nerve (10 mm gap)	A: autograft B: PLLA/ gelatin	–	(N.S.) –25 (A), –30 (B)	–	–	(N.S.) Muscle Fiber Diam. (μm): 45 (A), 40 (B); Collagen Fiber Area %: 5.2 (A), 5.5 (B)	–	($p < 0.05$) 85 (A), 70 (B)	–	–	24 weeks
Zheng et al (2021)[29]	144 adult male SD rats, 250 ± 20 g; Left sciatic nerve (5 mm gap)	A: autograft B: PLLA-aligned /0.25% pDNM gel	–	($p < 0.002$) –25 (A), –44.9 ± 4.5 (B)	–	–	–	–	–	–	–	8 weeks
Nerve Conduit with Cellular Factors												
Kaka et al (2017)[30]	30 adult male Wistar rats; Right sciatic nerve	B: PLGA C: PLGA + BMSCs	–	($p < 0.05$) –38 (B), –40 (C)	–	–	–	–	–	–	(N.S.) (hot water test, s) 41 (B), 40 (C)	8 weeks
Hu et al (2017)[31]	24 adult SD rats; Right sciatic nerve (10 mm gap)	B: conduit + ASCs C: conduit + FGF2-miR-218 ASCs		($p < 0.05$) –44.1 ± 3.1 (B), –34.7 ± 1.2 (C)	(Catwalk analysis) ($p < 0.05$) Mean stance time (s): 0.231 (B), 0.265 (C); ($p > 0.05$) Mean swing time (s): 0.391 (B), 0.289 (C)	–	–	–	–	–	–	10 weeks

(*Continued*)

https://doi.org/10.2147/IJN.S362144

Table 4 (Continued).

Paper	Animal		Functional Assessment								
	Species, Weight, Part of Incision	Experiment Group	Administration of Pain-Killer/ Antibiotics	Motor Function Analysis		Muscle Weight	Masson Trichrome Staining	Electrophysiological Examination			Sensory Recovery (HPL / PWL)	Duration
				SFI	Other			CMAP (mV)	NCV (m/s)	TL (ms)		
Das et al (2017)[32]	40 3-months-old female SD rats (250 g); Right sciatic nerve (10 mm gap)	P: normal B: PASF + SCs	Maintained on antibiotic (ceftriaxone) and NSAID (Meloxicam) for 5 d after surgery	−47 (B)	–	–	–	–	58 ± 2 (P), 50 ± 2.2 (B)	–	HPL (s): 163 ± 3.6 (P), 124 ± 2.5 (B)	48 weeks
Far-zamfar et al (2018)[33]	30 3-months-old healthy adult male Wistar rats (250–270 g); Right sciatic nerve (10 mm gap)	A: autograft B: conduit + hUSSCs	–	($p < 0.005$) −26.67 ± 3.66 (A), −53.6 ± 3.8 (B)	–	($p < 0.05$) (weight loss %) 5 (A), 17 (B)	(N.S.) Muscle bundles CSA: 1907 ± 67 (A), 1879 ± 41 (B)	(N.S.) 24 (A), 22(B)	–	–	($p < 0.05$) (HPL, s) 6.5 (A) 6.66 ± 0.96 (B)	14 weeks
Pereira dos Santos et al (2019)[34]	72 male Wistar rats (250 g); Right sciatic nerve (7 mm gap)	B: conduit only C: conduit + SHED		(N.S.) −85 (B, C); Group C showed faster recovering	($p < 0.05$) (Ladder Rung Test, error score) Quantitative: 10 (B), 15 (C); Qualitative: 5 (B), 6 (C)	($p < 0.05$) Soleus (g): 0.12 (B), 0.17 (C); ($p > 0.05$) Tibialis anterior (g): 0.36 (B), 0.32 (C)	–	–	–	–	–	4 weeks
Ma et al (2020)[35]	Male SD rats (230–250 g); Left sciatic nerve (17 mm gap)	A: autograft B: PCL/ PFTBA + PFTBA/SCs/ gelatin	–	(N.S.) −36 (A), −37.5 (B)	(N.S.) (Plantar test) Walking mean latency (s): 6 (A), 7 (B)	—	(N.S.) Ave. muscle fiber area %: 70 (A), 70 (B)	(N.S.) 50 (A), 47 (B)	(N.S.) 27 (A), 25 (B)	(N.S.) 1.35 (A), 1.5 (B)	–	12 weeks
Nerve Conduit with Non-Cellular Factors												
Suzuki et al (2017)[36]	40 male Wistar rats (180–220 g); Left sciatic nerve (crushed 5 mm distal from sciatic notch)	N: negative control B: PCL + MeCbl (MeCbl local)	–	($p < 0.05$) −20.6 ± 4.2 (N), −9.0 ± 2.0 (B),	–	–	–	($p < 0.05$) 19.5 ± 2.3 (N), 18.5 ± 1.5 (B)	($p < 0.01$) 28.2 ± 2.5 (N), 44.4 ± 2.8 (B)	(N.S.) 2.45 ± 0.08 (N), 2.27 ± 0.09 (B)	($p < 0.05$) (PWL, g) 117.8 ± 11.7 (N), 80 ± 7.6 (B)	6 weeks
Chang et al (2017)[37]	New Zealand white rabbits (3–3.5 kg); Sciatic nerve (15 mm gap)	A: autograft B: multi-channeled/ aligned nanofibers/ neurotrophic gradient (MC/ AN/NG)	–	–	–	(N.S.) (relative weight, %) 80 (A), 75 (B)	(N.S.) Muscle fiber Φ (μm): 51 (A), 50 (B) Ave. colla-gen fiber area (%): 8 (A), 8.5 (B)	($p < 0.05$) 4.8 (A), 4.2 (B)	($p < 0.05$) 46 (A), 35 (B)	–	–	24 weeks

Naseri Nosar et al (2017)[38]	20 3-month-old healthy adult male Wistar rats (250–270 g); Left sciatic nerve (10 mm gap)	B: conduit only C: conduit + CGNs	–	($p < 0.01$) –55.03 ± 3.16 (B), –34.23 ± 4.15 (C),	–	($p < 0.05$) (wet weight loss, %) 12.59 ± 4.18 (B), 4.18 ± 0.26 (C)	–	–	–	–	($p < 0.05$) (HPL, s) 7.67 ± 1.15 (B), 5.00 ± 1.00 (C)	60 days
Hong et al (2018)[39]	Male adult SD rats (270–330 g); Left sciatic nerve (clamped by 100 g force micro clamp for 10 s, 2 mm jaw width)	N: negative control B: NT-3 & BDNF in 2nd layer, PDGF in 3rd layer	–	($p < 0.001$) –38 (N), –5 (B)	–	–	–	–	–	–	($p < 0.001$) (PWL, g) 18 (N), 26.5 (B)	5 weeks
Far-zamfar et al (2018)[40]	16 3-month-old healthy adult male Wistar rats (250–270 g); Left sciatic nerve (10 mm gap)	A: autograft B: CA/ gelatin/ GBP6%	–	(N.S.) –51 ± 3.95 (A), –46.79 ± 2.05 (B)	–	(N.S.) (wet weight loss, %) 6.69 ± 0.47 (A), 5.89 ± 0.96 (B)	–	–	–	–	(N.S.) (HPL, s) 6.33 ± 0.58 (A), 6.67 ± 0.58 (B)	60 days
Xia et al (2018)[41]	Adult female SD rats (200–220 g); left sciatic nerve (10 mm gap)	A: autograft B: PLLA + NGF + VEGF	–	($p < 0.05$) –49.33 ± 1.21 (A), –64.81 ± 5.22 (B)	($p < 0.05$) SSI: –55.84 ± 2.04 (A), –70.59 ± 4.27 (B)	–	Recovery of muscle fiber structure in group A & E was better and similar to each other	–	($p < 0.05$) 38 ± 1.73 (A), 33.1 ± 1.51 (B)	–	–	12 weeks
Cheong et al (2019)[42]	9-week-old SD rats; Left sciatic nerve (15 mm gap)	A: autograft B: PLGA/ MAP-i	–	–	–	($p < 0.05$) (relative weight, %) 87.8 (A), 95.7 (B)	–	(N.S.) 15.75 ± 2.79 (A), 19.28 ± 2.47 (B)	–	(N.S.) 1.138 ± 0.108 (A), 1.075 ± 0.080 (B)	($p < 0.05$) (PWL, relative stimulus threshold, %) 82.9 (A), 95.4 (B)	8 weeks
Sayanagi et al (2019)[43]	51 male Wistar rats (180–220 g); Left sciatic nerve (10 mm gap)	A: autograft B: PGA-c/sheet	–	(N.S.) –74.9 ± 1.8 (A), –83.8 ± 6.2 (B)	($p < 0.05$) Isometric tetanic force (g): 116.6 ± 10.3 (A), 53.5 ± 18.1 (B)	($p < 0.01$) (wet weight, mg) 553.7 ± 35.0 (A), 305.5 ± 49.1 (B)	–	($p < 0.05$) 11.8 ± 1.4 (A), 4.3 ± 1.4 (B)	(N.S.) 40.0 ± 9.6 (A), 35.7 ± 5.1 (B)	($p < 0.01$) 2.99 ± 0.13 (A), 3.87 ± 0.24 (B)	($p < 0.05$) (PWL) 1.35 ± 0.19 (A), 1.51 ± 0.28 (B)	12 weeks
Rao et al (2020)[44]	SD rats (200–220 g); Right sciatic nerve (15 mm gap)	A: autograft B: conduit + ACG-KLT/NGI	–	($p < 0.05$) –50 (A), –57 (B)	–	($p < 0.05$) (wet weight ratio, %) 70 (A), 58 (B)	($p < 0.05$) Muscle CSA: 1500 (A), 1100 (B)	($p < 0.05$) 12.5 (A), 10 (B)	–	(N.S.) 1.5 (A), 2 (B)	–	12 weeks
Chen et al (2020)[45]	16 SD rats (150–200 g); Right sciatic nerve (15 mm gap)	A: autograft B: multi-layer (PCL + Fe_3O_4-MNPs + MLT)	160,000 units of penicillin were injected i.p. for infection prevention	(N.S.) –23.8 (A), –29.9 (B)	–	–	–	–	($p < 0.05$) 18.6 (A), 24.7 (B)	–	–	16 weeks

(*Continued*)

https://doi.org/10.2147/IJN.S362144

Table 4 (Continued).

Paper	Animal		Functional Assessment								
	Species, Weight, Part of Incision	Experiment Group	Administration of Pain-Killer/ Antibiotics	Motor Function Analysis		Muscle Weight	Masson Trichrome Staining	Electrophysiological Examination			Sensory Recovery (HPL / PWL)	Duration
				SFI	Other			CMAP (mV)	NCV (m/s)	TL (ms)		
Amini et al (2020)[46]	24 adult male Wistar rats (220–250 g); Left sciatic nerve (10 mm gap)	A: autograft B: P15L	Maintained on antibiotic (cefzolix) i.m. injection of 50 mg/kg after surgery	(N.S.) –41.34 ± 2.42 (A), –42.19 ± 9.0 (B)	–	($p < 0.01$) (wet weight, %) 75.83 ± 0.1 (A), 62.19 ± 2.5 (B)	($p < 0.001$) Collagen fiber area ave. %: 10 (A), 16 (B); ($p < 0.001$) Muscle fiber mean Φ (μm): 55 (A), 45 (B)	($p < 0.05$) 15.46 (A), 13.98 (B)	(N.S.) 18.03 (A), 17.17 (B)	(N.S.) 1.45 (A), 1.5 (B)	–	12 weeks
Sama-dian et al (2020)[47]	24 3-month-old healthy adult male Wistar rats (250–270 g); Left sciatic nerve (10 mm gap)	A: autograft B: PCL/ gelatin + PRP gelatin + Citi.	–	($p < 0.05$) –20 (A), –30.3 ± 1.9 (B)	–	(N.S.) (wet weight loss, %) 5 (A), 8.4 ± 1.3 (B)	–	–	–	–	(N.S.) (HPL, s) 5.3 ± 1.1 (A), 6.02 ± 1.0 (B)	12 weeks
Nerve Conduit with Combination Strategy (Cellular + Non-Cellular Factors)												
Jahro-mi et al (2020)[48]	35 adult male Wistar rats (4 months old, 240–280 g); Right sciatic nerve (10 mm gap)	A: autograft B: fibrin + SCs + nano-curcumin	–	(N.S.) –30 (A), –20 (B)	–	(N.S.) (wet weight loss, g) 1.5 (A), 1.2 (B)	–	–	–	–	(N.S.) (HPL, s) 6 (A), 4 (B)	12 weeks
Zhou et al (2020)[49]	45 male SD rats (200–250 g); Right sciatic nerve (10 mm gap)	A: autograft B: BMSCs + NGF + RCCS	Injections of meloxicam every 24 h or per requirement for 48 h following surgery	–79.0 ± 4.7 (A), –72.9 ± 10.4 (B)	–	($p < 0.05$) 57.5 ± 8.5 (A), 33.3 ± 3.4 (B)	–	8.3 ± 2.0 (A), 4.1 ± 0.6 (B)	29.6 ± 6.3 (A), 33.3 ± 2.7 (B)	–	–	12 weeks
Jahro-mi et al (2021)[50]	48 male Wistar rats (200–250 g); Left sciatic nerve (10 mm gap)	B: PLGA only C: PLGA + r-ADSC + AuNPs- & BDNF-CNPs + alginate		($p < 0.001$) –65 (B), –25 (C)	–	($p < 0.001$) (wet weight ratio, %) 40 (B), 76 (C)	($p < 0.01$) Muscle fibers Φ (μm): 13.02 ± 0.36 (B), 19.0 ± 0.90 (C)	–	–	–	–	12 weeks

Abbreviations: SFI, Sciatic Functional Index; CMAP, Compound Muscle Action Potential; NCV, Nerve Conduction Velocity; TL, Time Latency; HPL, Hot Plate Latency; PWL, Paw-Withdrawal Latency.

According to Table 5, only 1 out of the 39 studies did not provide any histological outcomes[38], while the others have adopted hematoxylin and eosin (H&E) staining, toluidine blue (TB) staining and transmission electron microscopes (TEM) for morphometric assessments, and various gene and protein expression for visualization of regenerative axons, SCs or inflammatory markers.

Studies will be compared by groups whereby the groups will be divided according to the duration of study. There are 2 groups: 5 studies in the group of 8 weeks and 16 studies in the group of 12 weeks, total 2 groups to be compared. Nineteen studies were not included in either of these 2 groups as they were not comparable due to lack of statistical analysis, incomplete assessments or unique methodology. The experimental groups within a study have been standardized as: autograft group (A), normal group (sham operation, without surgery; P), negative control group (injured nerve without treatment; N) and other treatment groups (B and C). The details of each group are as labeled in Table 4.

Within the group of 8 weeks, although Zhang et al[17] has shown significantly better functional outcomes to other groups, they did not provide the statistical significance of their histological study, thus was excluded from the discussion here. With respect to functional outcomes, both Song et al[13] and Moharrami Kasmaie et al[27] have shown no significant difference of nerve regeneration between experimental groups and the autograft group whilst Zheng et al[29] again showed that their nerve conduit was still inferior to autograft. Although Kaka et al[30] did not compare their results with autograft, they showed that the number and area of regenerated nerve fibers and blood vessels were larger with the presence of BMSCs. Cheong et al[42] had shown that functionalization with bio-functional peptides resulted in higher S100 (marker for SCs) and NF200 (marker for regenerated axons) fluorescence intensity relativity and number of myelinated axons in the experimental group compared to the autograft group. Both the studies from Kaka et al[30] and Cheong et al[42] showed us the potential of the strategies of stem cells and bio-functional peptides to be used in effective nerve regeneration.

For the group of 12 weeks, Zhang et al[14], Jing et al[18], Ma et al[35] and Samadian et al[47] have shown no significant difference between experimental groups and autograft group. Apart from the 4 above-mentioned studies, the regenerated nerves from other studies were still inferior than autograft, even with additional factors or combination strategies. Zhou et al[12] and Jahromi et al[50] have shown us that nerve conduit with aligned nanofibers or additional factors brought the superior nerve regeneration results to the one without aligned nanofibers or additional factors, which provided encouragement to the application of electrospun nanofibers or additional factors for the development of nerve guidance conduit for peripheral nerve regeneration.

We may observe the degradation of materials of nerve conduit through H&E staining as well, in which the residual materials can be recognized from the staining results. Nerve conduit should provide sufficient support to the nerve during the regeneration process. Hence it should not be fully degraded before the nerve regeneration has completed. Zhou et al[12] have mentioned that residual PPY polymers could still be observed after 12 weeks of implantation, which indicated that the polymer is suitable for nerve conduit fabrication as it will be gradually degraded throughout the nerve regeneration process.

Inflammation that occurs after a surgery will further be compounded by the presence of foreign component into the body. It can be observed by H&E staining, or by inflammatory protein markers expression. Xia et al[41] observed more inflammatory cells in the conduit group compared to the autograft group, although SCs proliferation, distribution, arrangement of nerve fibers and formation of new blood vessels in both groups were similar. Interestingly, Chen et al[45] have mentioned that MLT & Fe_3O_4-MNPs actuated the translation of macrophage phenotype from pre-inflammatory (M1) to anti-inflammatory (M2), which showed us the potential of adding anti-inflammatory drugs to the nerve conduit to reduce pain in animal models.

Although not being mentioned in Table 5, from the histological results, it was observed that the regenerative axons and SCs were able to grow parallel and along the alignment of electrospun fibers. Besides, higher density of regenerated nerve fibers, axons and SCs, less inflammation could also be observed in the aligned morphology. Conversely, random-oriented fibers showed lower density of nerve fibers and more inflammation. Thus, electrospun aligned fibers not only guide regeneration of axons and SCs in an orderly fashion, they also aid nerve repair in a healthier environment.

Biasness of Study

In order to look for alternatives of autograft for treatment of PNI, we should always compare our fabricated nerve conduit with the autograft, to give more appropriate evaluation findings, and to reveal how much the conduit is inferior to or close to the autograft. Besides a clearly stated sample size or capacity, such as the number of animals to be used in the research, it is important to indicate the transparency of a research study. Moreover, as mentioned above, statistical significance is extremely important and symbolic

Table 5 Comparison of Gene and Protein Expression and Morphometric Assessment Outcome of All Studies

Ref.	Morphometric Assessment			Gene and Protein Expression		Remarks
	H&E	Semi-Thin Section	TEM	Data	Interpretation	
Nerve Conduit with Micro- or Nano-Fiber Only						
Zhou et al (2016)[12]	Structures of myelinated fibers of PELA-PPY scaffold similar to autograft	Amount of positive labeled cells similar to autograft	($p < 0.05$) Total no. of regenerated myelinated fibers: 79 (A), 25 (B), 78 (C) Myelin thickness (μm): 0.6 (A), 0.35 (B), 0.65 (C); Axon diam. (μm): 1.6 (A), 0.8 (B), 1.6 (C)	($p < 0.05$) No. of positive GFAP/area: 165 (A), 40 (B), 140 (C); No. of positive NF/area: 165 (A), 120 (B), 160 (C); No. of positive S100/area: 89 (A), 40 (B), 90 (C); No. of positive Laminin/area: 165 (A), 40 (B), 140 (C); No. of positive BrdU/area: 130 (A), 50 (B), 90 (C)	GFAP: marker for cytoskeletal reorganization, myelination maintenance & cell adhesion; NF: marker for regenerative axons; S100: marker for Schwann cells; Laminin: an active part of basal lamina, marker for ad-hesion & migration of cells; BrdU: marker for detection of proliferative cells	Residual PPY polymers in regenerated nerves
Song et al (2016)[13]	–	(N.S.) Ave. axon diam. (μm): 3.25 (A), 3.0 (B); Nerve fiber diam. (μm): 6.5 (A), 6 (B); No. of nerve fibers: 10,000 (A), 8000 (B)	(N.S.) Myelin thickness (μm): 0.6 (A), 0.65 (B);	(N.S.) S100 PAP (%): 40 (A), 20 (B), 35 (C); NF160 PAP (%): 42 (A), 23 (B), 40 (C)	S100: marker for Schwann cells; NF160: marker for regenerative axons	More host-derived SC entered middle of NGC when ES applied where more NF160+ axons were observed
Zhang et al (2016)[14]	–	(N.S.) Diam. of nerve fibers (μm): 4.55 ± 0.12 (A), 4.43 ± 0.14 (B); Myelin thickness (μm): 0.96 ± 0.06 (A), 0.92 ± 0.07 (B)	Formation of regenerated myelinated fibers occurred, with a structure of compact & uniform on C	–	Positive expression of NF200 (marker for regenerative axons); Regenerated axons in C similar to A	–
Du et al (2017)[15]	Oriented fibrin fibers still existed at week 2	Denser cells on group B, similar to autograft	($p < 0.05$) Myelinated nerve fiber density (/mm2): 55,000 (A), 46,000 (B); Diam. of myelinated nerve fiber (μm): 370 (A), 350 (B); Thickness of myelin sheath (μm): 75 (A), 65 (B)	–	Positive expression of S100 & NF200, regenerated tissues were observed; Higher axonal regeneration rate in aligned fibers; Group A & B showed better density of regenerated nerve fibers	–
Sun et al (2017)[16]	Regenerated nerves in group B approximate to A	(N.S.) No. of positive SCs (/1000 μm^2): 620 (A, B); Myelin PAP (%): 61 (A), 59 (B)	($p < 0.01$) Axon diam. (μm): 9 (A), 5 (B); ($p < 0.05$) Myelin thickness (μm): 1.0 (A), 0.75 (B)	(N.S.) S100 PAP (%): 24 (A), 26 (B); ($p < 0.05$) NF200 PAP (%): 17 (A), 15 (B); GFAP PAP (%): 18 (A), 15 (B);	S100: marker for Schwann cells; NF200: marker for regenerative axons; GFAP: marker for cytoskeletal reorganization, myelination maintenance & cell adhesion	–

Zhang et al (2018)[17]	Regenerated nerve fibers of A similar to normal nerve fibers; SCs were found in regenerate nerves	–	–	–	Positive expression of S100, NF200 & PGP9.5; Confirmed the regeneration of myelinated nerve fibers, growth of SCs on longitudinal slides & regeneration of axons;	–
Jing et al (2018)[18]	–	(N.S.) Nerve fibers diam. (μm): 7 (A), 6.2 (B); Density of nerve axons (no./mm^2): 23,750 (A), 27,500 (B); Myelin thickness (μm): 0.9 (A), 0.82 (B)	–	–	Positive expression of NF & S100 (marker for regenerative axons & Schwann cells); Noticeable amounts of S100 could be identified in both A & B	–
Sun et al (2019)[19]	Size & distribution of nerve axons were slightly more uniform in C	(N.S.) No. of positive SCs (/1000 μm^2): 620 (A), 580 (B), 600 (C); Myelin PAP (%): 62 (A), 38 (B), 60 (C)	($p < 0.01$) Axon diam. (μm): 10 (A), 5 (B), 7 (C); ($p < 0.05$) Myelin thickness (μm): 1.0 (A), 0.6 (B), 0.8 (C)	–	Positive expression of S100 & NF200; Group A & C showed stronger expression of S100 & NF200; Fluorescent cells & axons count of group C was much higher	–
Farzamfar et al (2019)[20]	Nerve fibers were well-arranged & fibrosis or inflammatory cell infiltration were not seen in group B, which similar to group A	–	–	–	–	–
Lopez et al (2019)[21]	–	($p < 0.05$) Total axon count: 1072 ± 123.80 (B), 1769 ± 672 (C); Collagen PAP (%): 0.891 ± 0.023 (B), 0.748 ± 0.054 (C)	($p < 0.05$) Myelin thickness (μm): 0.712 ± 0.293 (B), 0.858 ± 0.26 (C); ($p = 0.116$) Axon diam. (μm): 1.56 ± 0.72 (B), 1.84 ± 0.75 (C); ($p = 0.753$) G ratio: 0.516 ± 0.177 (B), 0.502 ± 0.121 (C)	–	–	–
Yen et al (2019)[22]	Group A & D had the largest nervous tissue areas; Myelin sheaths in group D were still growing with a few newborn blood vessels; Blood vessel no.: 0.30 ± 0.48 (B), 1.50 ± 1.08 (C)	Nerve fiber no.: 793.1 ± 205.0 (B), 1572.8 ± 202.0 (C); Nerve fiber diam. (μm): 0.22 ± 0.06 (B), 0.27 ± 0.08 (C); Medial nerve area (μm^2): 2894.51 ± 111.12 (B), 12,483.14 ± 4.43 (C)	Myelin sheath thickness (μm): 0.1 ± 0.01 (B), 0.12 ± 0.02 (C);	–	Positive expression of CD4 & S100; Group C showed more S-100 staining & were barely stained with CD4; Group B were stained with more CD4 (marker for T-helper cells, indicated more inflammation)	–

(*Continued*)

https://doi.org/10.2147/IJN.S362144

Table 5 (Continued).

Ref.	Morphometric Assessment			Gene and Protein Expression		Remarks
	H&E	Semi-Thin Section	TEM	Data	Interpretation	
Wang et al (2019)[23]	–	(N.S.) No. of positive SCs (/1000 μm^2): 680 (A), 640 (B); Myelin PAP (%): 68 (A), 70 (B)	($p < 0.05$) Axon diam. (μm): 6 (A), 5 (B)	(N.S.) S100 PAP (%): 48 (A), 24 (B), 46 (C); NF200 PAP (%): 50 (A), 22 (B), 44 (C);	S100: marker for Schwann cells; NF200: marker for regenerative axons	–
Neshat et al (2020)[24]	($p < 0.05$) Diam. of myelinated fibers (μm): 3.05 ± 0.5 (B), 4.89 ± 1.4 (C); Nerve fiber area (μm2): 9.73 ± 4.12 (B), 23.94 ± 8.35 (C); No. of myelinated fibers: 65 (B), 193 ± 7.4 (C)	–	–	–	Positive expression of S100; Confirmed the presence of SCs in vicinity of the myelin sheath & through nerve fibers	–
Wang et al (2020)[25]	Positive degrees of HE in group C & D > B; No obvious infiltration of inflammatory cells, cellular edema & steatosis in all groups;	($p < 0.05$) No. of positive SCs (/1 mm^2): 7000 (A), 5500 (B); (N.S.) Myelin PAP (%): 78 (A), 32 (B), 34 (C), 80 (D)	–	($p < 0.01$) S100β PAP (%): 18 (A), 14 (B); NF200 PAP (%): 33 (A), 25 (B); CD31 PAP (%): 1.8 (A), 1.3 (B); Microvessel density (MVD/mm^2): 55 (A), 43 (B);	CD31: marker for vascular differentiation; Multichannel NGC supported higher SCs density & remyelination	Multichannel NGC enhanced neovascularization
Zhang et al (2020)[26]		($p < 0.05$) Diam. of myelinated fibers (μm): 5.5 (A), 4.5 (B); Myelinated axon area (μm^2): 25 (A), 16 (B); Density of myelinated nerve fibers (no./mm^2): 16,000 (A), 12,000 (B)	($p < 0.05$) Myelin thickness (μm): 2.7 (A), 1.6 (B)	MBP PAP (%): 13 (A), 9.5 (B); S100 PAP (%): 14 (A), 11.5 (B); NF200 PAP (%): 19.5 (A), 13 (B); qPCR: higher Krox20 & GFAP expression in group B than A; levels of BDNF, VEGFα & Zeb2 showed no difference among groups	MBP: marker for myelination; Krox20: highly expressed in migrating neural crest cells; GFAP: marker for cytoskeleton, myelination & cell adhesion; BDNF: marker for prolifera-tion /differentiation of neural stem/progenitor cells; VEGFα: marker for angiogenic and neurotrophic factor in nerve regeneration; Zeb2: found in tissues differ-rentiated from neural crest	–
Moharrami Kasmaie et al (2021)[27]	Substantial host cell infiltration into scaffold; Revascularization & good integration of B with host tissue	sGAG: Host's cells secreted ECM between scaffold layers; LFB: myelinated axons in group B	–	(N.S.) SCs no.: 97.33 ± 9.83 (P), 70.5 ± 16.3 (A), 47.5 ± 23.38 (B); ($p < 0.05$) Axons no.: 142 ± 39.28 (P), 74.83 ± 25.52 (A), 19.33 ± 5.68 (B)	Schwann cells number & axons number were confirmed by positive expression of S100 & NF200	–

Niu et al (2021)[28]	–	Large number of myelinated nerve fibers develop; Scaffold extensively degraded, regenerated epineurium tissue group A is thicker	(N.S.) Myelin sheath diam. (μm): 4.5 (A), 4.3 (B); Myelin thickness (μm): 0.9 (A), 0.8 (B)	S100B PAP (%): 8.5 (A), 6.5 (B); NF200 PAP (%): 30 (A), 27 (B)	S100B: marker for Schwann cells; NF200: marker for regenerative axons	–
Zheng et al (2021)[29]	Group A showed most promising recovery in nerve fiber continuity; nerve fiber regrowth was closely packed & highly ordered in group B	($p < 0.002$) Count of axons: 135 (A), 120 (B); Diam. of myelinated fibers (μm): 4.7 (A), 3.5 (B); Myelin thickness (μm): 0.85 (A), 0.75 (B)	–	–	–	–
Nerve Conduit with Cellular Factors						
Kaka et al (2017)[30]	($p < 0.05$) No. of nerve fibers (1000 μm^2): 10.5 (B), 14 (C); Area of blood vessels: 1900 (B), 2500 (C)	–	–	–	–	–
Hu et al (2017)[31]	($p < 0.05$) CSA of regenerated nerve (mm^2): 9.79 (B), 12.06 (C)	–	–	–	S100 staining confirmed regeneration of nerve fibers	Scaffolds integrated into host tissue, no dislocation, appeared healthy
Das et al (2017)[32]	Showed cellular recruitment inside PASF NGC; SF NGC showed less cellular migration inside nerve gap	–	Lumen of PASF + SCs NGC revealed thick deposition of myelin in a lamellar fashion similar to normal nerves	–	–	In vivo intracutaneous toxicity study: did not induce formation of erythema or edema; No dislocation or deformation of implanted NGC
Farzamfar et al (2018)[33]	Group C: well-arranged nerve fibers, intact myelin sheath, negligible vacuolation & edema	–	–	–	–	No signs of hematoma or infection were observed at implantation site
Pereira dos Santos et al (2019)[34]	–	($^{p} < 0.05$) Myelinated fiber Φ (μm): 4.8 (B), 4.2 (C); Axon Φ (μm): 3.8 (B), 3.5 (C); Myelin sheath thickness (μm): 0.9 (B), 0.7 (C); Density of myelinated fibers (mm2): 25,000 (B), 29,000 (C)	–	–	–	–

(*Continued*)

https://doi.org/10.2147/IJN.S362144 DovePress

Table 5 (Continued).

Ref.	Morphometric Assessment			Gene and Protein Expression		Remarks
	H&E	Semi-Thin Section	TEM	Data	Interpretation	
Ma et al (2020)[35]		(N.S.) Recovery ratio of regenerated axons PAP (%): 87 (A), 85 (B); No. of myelinated axons (104/mm^2): 1.35 (A), 1.25 (B)	(N.S.) Φ of myelinated axons (μm): 4.25 (A), 4 (B); G-ratio: 0.55 (A), 0.6 (B)	–	S100, NF160 staining showed more regenerated nerve fibers in group B	Fluoro-Gold (FG) retrograde tracing: no. of FG-labeled motor neurons in spinal cord & sensory neurons in DRGs peaked on & high levels of neuronal regeneration into distal stumps of group A & B
Nerve Conduit with Non-Cellular Factors						
Suzuki et al (2017)[36]	–	–	–	(N.S.) Axons Φ (μm): 3.41 ± 0.11 (P), 2.70 ± 0.06 (B); No. of axons (/mm^2): 2843 ± 68 (N), 2733 ± 142 (B); ($p < 0.001$) Myelinated axon ratio (%): 85.0 ± 0.9 (N), 91.0 ± 0.8 (B)	–	($p < 0.001$) Plasma concentration of MeCbl (ng/mL): 1.50 ± 0.07 (N), 1.73 ± 0.05 (B)
Chang et al (2017)[37]	–	–	($p < 0.05$) Axons Φ (μm): 9 (A), 8 (B); Myelin sheath thickness (μm): 3.5 (A), 3.3 (B); Myelinated fibers Φ (μm): 15 (A), 14.2 (B)	–	–	–
Naseri Nosar et al (2017)[38]	–	–	–	–	–	–
Hong et al (2018)[39]	–	–	–	($p < 0.05$) Tuj1 expression (a.u.): 0.35 (N), 0.85 (B); MAP2 expression (a.u.): 1.05 (N), 0.85 (B)	Tuj1: marker for neurons from early stage of neural differentiation; MAP2: marker for perikaryal & dendrites of neuronal cells	–
Farzamfar et al (2018)[40]	(N.S.) Muscular fiber CSA (mm^2): 1850 (A), 1800 (B)	–	–	–	–	–
Xia et al (2018)[41]	SCs proliferation, distribution, arrangement of nerve fibers, formation of new blood vessels in group B similar to A	–	–	–	Group B exhibited higher positive staining of NF-M (marker for axons) than those in other groups	More inflammatory cells could be observed between fibers in group B

Cheong et al (2019)[42]	Group B had the densest & largest axon- & endoneurium-like structures close to group A	–	–	($p < 0.05$) Fluorescence intensity relativity: 100 (A), 145 (B); No. of myelinated axon relativity: 100 (A), 160 (B)	Showed fluorescence intensity of combination of S100 & NF200	
Sayanagi et al (2019)[43]	–	($p < 0.05$) Myelinated axon area (%):12.0 ± 1.0 (A), 10.9 ± 1.5 (B)	($p < 0.001$) G-ratio: 0.64 ± 0.004 (A), 0.72 ± 0.002 (B)	($p < 0.05$) Axon numbers (/mm^2): 22,714 ± 1254 (A), 20,640 ± 729 (B); Myelinated axons (%): 97.2 ± 0.6 (A), 93.8 ± 2.1 (B)	Positive expression of MBP (marker for myelination), NF200	Proportion of axons with a larger perimeter was greater in group B
Rao et al (2020)[44]		($p < 0.05$) Myelinated nerve fibers density (/mm^2): 12500 (A), 11000 (B)	($p < 0.05$) Myelinated axons Φ: 7.5 (A), 6.25 (B); Myelin sheath thickness: 1.20 (A), 0.95 (B)	–	CD31 (marker for vascular differentiation), NF200 staining – Greater nerve fiber regeneration & no. of vessels in group B; VEGF (marker for endothelial cell proliferation), GAP43 (marker for axonal growth) Western blot – higher expression in group B	FG retrograde tracing (N.S.) – No. of FG-positive motor neurons in spinal anterior horns: 470 (A), 430 (B); ($p < 0.05$) – No. of FG-positive sensory neurons in DRGs: 420 (A), 380 (B)
Chen et al (2020)[45]	Regenerated nerve: group B showed fewer vacuolar defects, structures were quite denser & organized; myelinated axons from both groups were more uniform than group A; (N.S.) Ave. muscle fibers Φ (μm): 32.05 (A), 33.84 (B)	(N.S.) Ave. axon Φ (μm): 3.64 (A), 3.30 (B); ($p < 0.05$) Mean thickness of myelin sheath (μm): 0.65 (A), 1.02 (B)	–	($p < 0.05$) Relative S100 level: 2.6 (A), 1.5 (B); Relative CD68 level: 0.9 (A), 0.4 (B); Relative CD206 level: 3 (A), 2.5 (B); (N.S.) Relative NF200 level: 1.08 (A), 1.15 (B); Relative MBP level: 1.6 (A), 1.65 (B); Relative IL-6 level: 0.9 (A), 0.86 (B); Relative IL-10 level: 1.4 (A), (B); ($p < 0.01$) Relative β-tubulin level: 2.0 (A), 1.6 (B); Relative vimentin level: 1.65 (A), 1.0 (B)	CD68: marker for M1 macrophage; CD206: marker for M2 macrophage; IL-6: marker for inflammation; IL-10: anti-inflammatory cytokine; β-tubulin: marker for regenerative axons; Vimentin: marker for activated fibroblasts (PCL) nanofibrous layers effectively reduced fibrosis and soft tissue infiltration, thus preventing scar formation	MLT & Fe3O4-MNPs actuated translation of macrophage phenotype from pre-inflammatory (M1) to anti-inflammatory (M2)
Amini et al (2020)[46]	Morphology of P15L was similar to autograft	(N.S.) Mean Φ of myelinated nerve fibers (μm): 7.2 ± 0.1 (A), 6.86 ± 0.7 (B); Mean Φ of myelinated axons (μm): 4.7 ± 0.2 (A), 4.7 ± 0.5 (B); Myelin sheath thickness (μm): 2.6 ± 0.1 (A), 2.3 ± 0.1 (B); ($p < 0.05$) G-ratio (μm): 0.63 ± 0.01 (A), 0.69 ± 0.02 (B)		(N.S.) S100 intensity (%): 95 (A), 90 (B); Map2 intensity (%): 80 (A), 75 (B); Axon number (%): 95 (A), 90 (B); ($p < 0.05$) βIII-Tubulin intensity (%): 80 (A), 65 (B); Nestin intensity (%): 90 (A), 80 (B)	MAP2: marker for perikaryal & dendrites of neuronal cells; Nestin: marker for axonal growth	–

(*Continued*)

https://doi.org/10.2147/IJN.S362144 DovePress

Table 5 (Continued).

Ref.	Morphometric Assessment			Gene and Protein Expression		Remarks
	H&E	Semi-Thin Section	TEM	Data	Interpretation	
Samadian et al (2020)[47]	(N.S.) Muscle fiber area (mm2): 2350 (A), 1900 (B); Nerve fiber arrangement was similar to healthy tissue in group A; mild vacuolation was observed in group B; Muscular fibers regenerated with negligible degree of fibrosis & muscular shrinkage	–	–	–	–	No sign of fibrosis or inflammatory cell infiltration
Nerve Conduit with Combination Strategy (Cellular + Non-Cellular Factors)						
Jahromi et al (2020)[48]	Group B showed complete degradation of NGC, neovascularization, without any inflammatory responses or remaining vacuolation area	–	–	($p < 0.05$) Nerve fiber count: 3579.6 ± 45.90 (A), 2760 ± 60.08 (B); Vessel count: 284 ± 11.76 (A), 273 ± 12.80 (B)	More myelinated nerve in group B; Mean NF-200 expression % significantly increases in group B;	
Zhou et al (2020)[49]	–	($p < 0.05$) No. of remyelinated axons: 10,588 ± 2539 (A), 6091 ± 877 (B)	–	–	–	–
Jahromi et al (2021)[50]	–	($p < 0.01$) Nerve fibers Φ (μm): 4.76 ± 0.25 (B), 6.45 ± 0.31 (C); Ave. no. of myelinated axon (/field): 14.2 ± 1.05 (B), 22.1 ± 1.1 (C)	($p < 0.05$) G-ratio: 0.42 ± 0.02 (B), 0.45 ± 0.02 (C); (N.S.) Myelinated axons Φ (μm): 2.03 ± 0.15 (B), 2.9 ± 0.06 (C); Myelin sheath thickness (μm): 2.72 ± 0.24 (B), 3.52 ± 0.31 (C)	($p < 0.001$) MBP intensity (%): 170 (B), 130 (C); NF-200 intensity (%): 115 (B), 225 (C); S100 intensity (%): 200 (B), 230 (C); (qRT-PCR, relative expression, N.S.) GFAP: 0.82 (B), 0.96 (C); ($p < 0.001$) Nestin: 1.15 (B), 2.5 (C)	MBP: marker for myelination; GFAP: marker for cytoskeleton, myelination & cell adhesion; Nestin: marker for axonal growth	–

Abbreviations: PAP, Positive Area Percentage; GFAP, Glial Fibrillary Acidic Protein; NF, Neurofilament; PGP, Protein Gene Product; BDNF, Brain Derived Neurotrophic Factor; VEGF, Vascular Endothelial Growth Factor; MBP, Myelin Basic Protein; MAP, Microtubule-Associated Protein; GAP, Growth-Associated Protein.

to a randomized study. It indicates the statistical relationship between randomized subjects, and visualizes the results through a simple index, allowing readers to understand the results of comparison and efficacy of specific nerve conduit intuitively. Furthermore, for studies using cells for additional factors, the passage number and number of cells to be seeded on conduit should be clearly stated. It is because cells at different developing stage may present different performances, which may have a huge impact on the studies.

However, according to Tables 2, 4 and 5, it was found that some of the studies: did not compare the efficacy of nerve conduit with autograft; did not clearly state their sample size, passage number of cells and numbers of cells to be seeded on conduit; and lastly the statistical analysis has not been done; which those "non-transparent" studies may lead to the lack of objectivity, and the decrease of reliability.

Studies are not without limitations. However, these limitations may drive the development of future studies, to fabricate better nerve conduits. Although some studies have fabricated nerve conduits that are reported to be at par with autograft, in general most were found to be inferior to autograft, even with added cellular or non-cellular factors. This may be due to the difficulty to mimic the unique microstructure of native nerves by conduits, and the lack of integrated delivery systems for growth factors or facilitating cells that limit the nerve repair function of the nerve conduits. The majority of the researches were of short duration, resulting in insufficient time for recovery of the injured nerve which may also contribute to a poorer outcome of the nerve conduit.

Conclusion

Electrospinning techniques produce nerve conduit that consists of aligned fibers which have been shown to produce better results compared to random fibers. Additionally, the alignment of the nerve conduit may help the orientation and attachment of additional factors such as cells, NFs, drugs and bio-functional peptides, which further extended the potentials and usage of a nerve conduit (Figure 2).

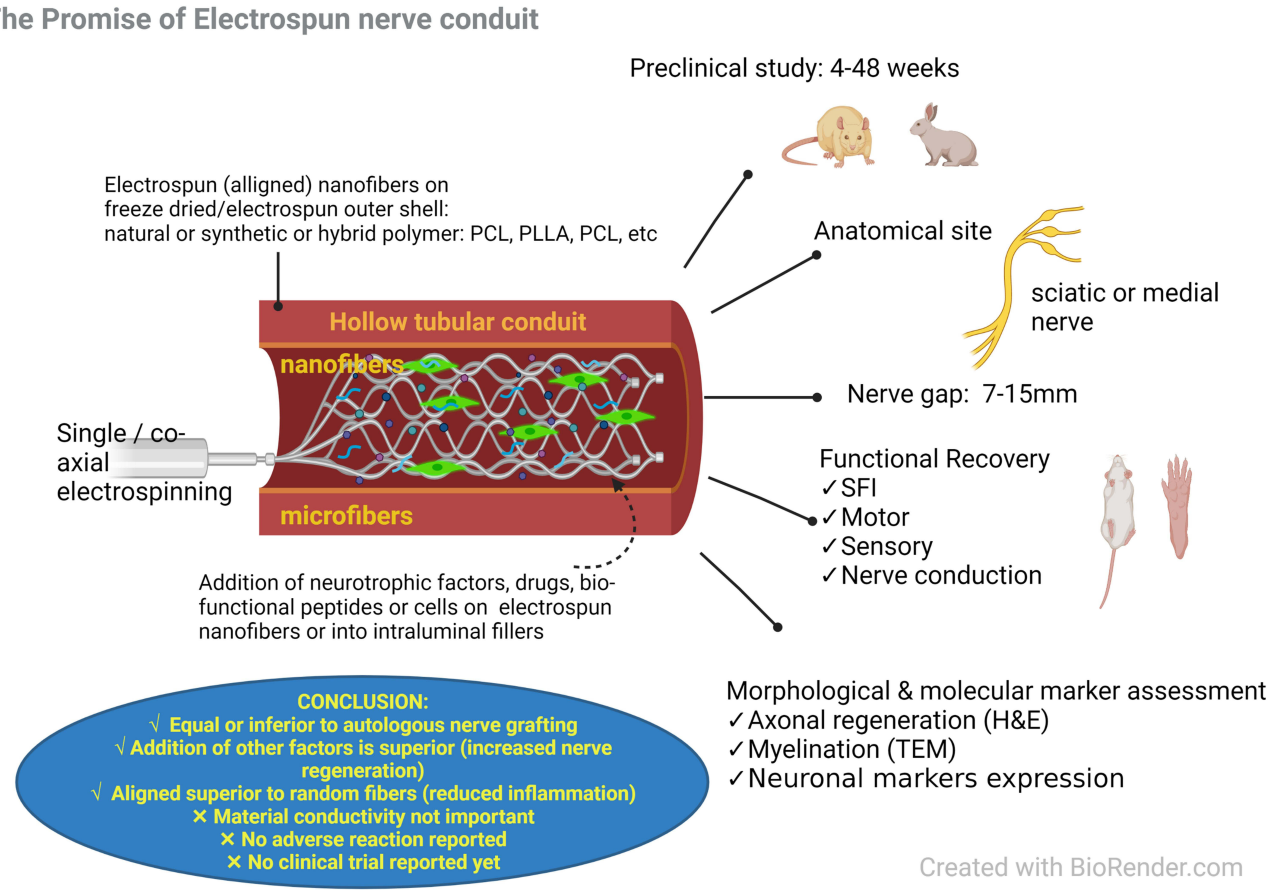

Figure 2 Schematic illustration of the promise of electrospun nerve conduit.

After a series of comparison, the most popular material for electrospun nerve conduit was PCL and PLLA. These two materials have shown better results compared to others and can be considered as the more suitable materials for fabrication of a nerve conduit. From Table 1, we found that conductivity of a nerve conduit was not significant to improvement in nerve regeneration and, thus, not a necessary indicator to be tested.

Based on Tables 1–5, the paradigm of development of electrospun nerve conduit has been switched from simple nano- or micro-fibers conduit to functionalization of a conduit using combination factors. Attempts are made to maximize the advantages of additional factors, with more complicated and complete strategy, to complement the deficiency of only a single factor. Although most of these studies with additional factors have shown better outcome compared to those without, they are still unable to demonstrate a superior result compared to autograft. The addition of stem cells, NFs, drugs or bio-functional peptides although optional, have potential to accelerate the nerve repairing procedure, and provide an environmental guidance for nerve regeneration. Furthermore, functionalization with antibiotics would be advantageous in a setting of an open wound in preventing surgical site infection and improving wound healing.[105]

Further Study

Studies on development of electrospun nerve conduit are still at the preclinical phase. There are many potentials awaiting to be explored, and further studies should continue until the best strategy has been found. There are other drugs or materials such as graphene and boron nitride that are used on other nerve conduit which have not been explored in electrospun conduits.[106,107] Aside from basic evaluation of the performance of in vivo implanted nerve conduit, researchers should perform molecular and cellular study to elucidate the effects of nerve conduit on facilitating better fascicle alignment, decreasing scarring, reducing inflammation and protecting fascicles from mechanical deformations.

There are only a few current literatures to show that electrospun nerve conduits are superior to autograft and further researches manipulating various parameters may not alter this fact. Researchers should consider accepting the fact that tissue engineered nerve conduit may never be at par with autograft and commence clinical trials where we will have a better understanding of its action in the human body.[108] The ability to avoid harvesting a donor nerve, thus, preventing donor site morbidity may ameliorate any disadvantages of a nerve conduit.

The logistic aspect of the commercialized product must also be considered. Stem cells harvested from the patient have to be factored in and this undoubtedly would affect the cost. Furthermore, the need to culture cells will also affect timing of surgery from the initial injury which could inherently impact the outcome of nerve regeneration.

Abbreviations

PNI, peripheral nerve injury; ECM, extracellular matrix; NS, nano-sponge; PELA, poly(D,L-lactide)-co-poly(ethylene glycol); PPY, polypyrrol; PLCL, poly(L-lactic acid-co-ε-caprolacton); SF, silk fibroin; CL, collagen; PHBV, poly (3-hydroxybutyrateco-3-hydroxyvalerate); PEO, polyethylene oxide; PLGA, poly(lactide-co-glycolide); PCL, polycaprolactone; CNF, carbon nanofiber; ApF, Antheraea pernyi silk fibroin; PLATMC, poly(lactide-co-trimethylene carbonate); PLLA, poly(L-lactic acid), SPI, gelatin, soy protein isolate; PLLA-TMC, poly(L-lactic acid-co-trimethylene carbonate); PASF, polyaniline-silk fibroin; PFTBA, perfluorotributylamine; CA, cellulose acetate; MAP, mussel adhesive proteins; PGA, polyglycolic acid; MWC, multi-wall carbon; SCs, Schwann cells; CNTs, carbon nanotubes; BMSCs, bone marrow stromal cells; ASCs, adipose-derived stem cells; NSCs, neural stem cells; iPSCs-NCSCs, induced pluripotent stem cells–neural crest stem cells; MSCs, mesenchymal stem cells; miRNA, microRNA; FGF, Fibroblast Growth Factor 2; NFs, neurotrophic factors; GFs, growth factors; EGF, epidermal growth factor; IGF, insulin-like growth factor; bFGF, basic fibroblast growth factor; PD, Parkinson's disease; CTC, citicoline; MeCbl, methylcobalamin; SFI, sciatic functional index; HPL, hot plate latency; PWL, paw withdrawal latency; MT, Masson Trichrome; CMAP, compound muscle action potential; NCV, nerve conduction velocity; TL, time latency of compound muscle action potential; hUSSCs, human unrestricted somatic stem cells.

Acknowledgments

The study is supported by research grant provided by Universiti Kebangsaan Malaysia (GUP-2019-084) and the Faculty of Medicine (FF-2021-151).

Disclosure

Prof. Dr Min Hwei Ng reports a patent PI 2019007825 pending to UKM. The authors declare no other conflicts of interest.

References

1. Daly W, Yao L, Zeugolis D, Windebank A, Pandit A. A biomaterials approach to peripheral nerve regeneration: bridging the peripheral nerve gap and enhancing functional recovery. *J R Soc Interface*. 2011;9:202–221. doi:10.1098/rsif.2011.0438
2. Tuturov AO. The role of peripheral nerve surgery in a tissue reinnervation. *Chin Neurosurg J*. 2019;5. doi:10.1186/s41016-019-0151-1
3. Chiono V, Tonda-Turo C. Trends in the design of nerve guidance channels in peripheral nerve tissue engineering. *Prog Neurogibol*. 2015;131:87–104. doi:10.1016/j.pneurobio.2015.06.001
4. Dodla MC. *Peripheral Nerve Regeneration*. Elsevier Inc.; 2011.
5. Hoben GM, Ee X, Schellhardt L, et al. Increasing nerve autograft length increases senescence and reduces regeneration. *Plast Reconstr Surg*. 2018;142(4):952–961. doi:10.1097/PRS.0000000000004759
6. Lovati AB, D'Arrigo D, Odella S, Tos P, Geuna S, Raimondo S. Nerve repair using decellularized nerve grafts in rat models. A review of the literature. *Front Cell Neurosci*. 2018;12:1–20. doi:10.3389/fncel.2018.00427
7. Cui T, Yan Y, Zhang R, Liu L, Xu W, Wang X. Rapid prototyping of a double-layer polyurethane-collagen conduit for peripheral nerve regeneration. *Tissue Eng Part C Methods*. 2009;15(1):1–9. doi:10.1089/ten.tec.2008.0354
8. Sulong AF, Hassan NH, Hwei NM, et al. Collagen-coated polylactic-glycolic acid (PLGA) seeded with neural-differentiated human mesenchymal stem cells as a potential nerve conduit. *Adv Clin Exp Med*. 2014;23(3):353–362. doi:10.17219/acem/37125
9. Bhardwaj N, Kundu SC. Electrospinning: a fascinating fiber fabrication technique. *Biotechnol Adv*. 2010;28:325–347. doi:10.1016/j.biotechadv.2010.01.004
10. Quan Q, Meng HY, Chang B, et al. Aligned fibers enhance nerve guide conduits when bridging peripheral nerve defects focused on early repair stage. *Neural Regen Res*. 2019;14:903–912. doi:10.4103/1673-5374.249239
11. Zou Y, Qin J, Huang Z, Yin G, Pu X, He D. Fabrication of aligned conducting PPy-PLLA fiber films and their electrically controlled guidance and orientation for neurites. *ACS Appl Mater Interfaces*. 2016;8:12576–12582. doi:10.1021/acsami.6b00957
12. Zhou ZF, Zhang F, Wang JG, et al. Electrospinning of PELA/PPY fibrous conduits: promoting peripheral nerve regeneration in rats by self-originated electrical stimulation. *ACS Biomater Sci Eng*. 2016;2(9):1572–1581. doi:10.1021/acsbiomaterials.6b00335
13. Song J, Sun B, Liu S, et al. Polymerizing pyrrole coated poly(l-lactic acid-co-+-caprolactone) (PLCL) conductive nanofibrous conduit combined with electric stimulation for long-range peripheral nerve regeneration. *Front Mol Neurosci*. 2016;9(117):1–13. doi:10.3389/fnmol.2016.00117
14. Zhang M, Lin W, Li S, et al. Application and effectiveness evaluation of electrostatic spinning PLGA-silk fibroin-collagen nerve conduits for peripheral nerve regeneration. *J Nanosci Nanotech*. 2016;16(9):9413–9420. doi:10.1166/jnn.2016.11906
15. Du J, Liu J, Yao S, et al. Prompt peripheral nerve regeneration induced by a hierarchically aligned fibrin nanofiber hydrogel. *Acta Biomater*. 2017;55:296–309. doi:10.1016/j.actbio.2017.04.010
16. Sun B, Zhou Z, Wu T, et al. Development of nanofiber sponges-containing nerve guidance conduit for peripheral nerve regeneration in vivo. *ACS Appl Mater Interfaces*. 2017;9:26684–26696. doi:10.1021/acsami.7b06707
17. Zhang XF, Liu HX, Ortiz LS, Xiao ZD, Huang NP. Laminin-modified and aligned poly(3-hydroxybutyrateco-3-hydroxyvalerate) /polyethylene oxide nanofibrous nerve conduits promote peripheral nerve regeneration. *J Tissue Eng Regen Med*. 2018;12:e627–e636. doi:10.1002/term.2355
18. Jing W, Ao Q, Wang L, et al. Constructing conductive conduit with conductive fibrous infilling for peripheral nerve regeneration. *Chem Eng J*. 2018;345:566–577. doi:10.1016/j.cej.2018.04.044
19. Sun B, Zhou Z, Li D, et al. Polypyrrole-coated poly(l-lactic acid-co-ε-caprolactone)/silk fibroin nanofibrous nerve guidance conduit induced nerve regeneration in rat. *Mater Sci Eng C*. 2019;94:190–199. doi:10.1016/j.msec.2018.09.021
20. Farzamfar S, Salehi M, Tavangar SM, et al. A novel polycaprolactone/carbon nanofiber composite as a conductive neural guidance channel: an in vitro and in vivo study. *Prog Biomater*. 2019;8:239–248. doi:10.1007/s40204-019-00121-3
21. Lopez J, Xin K, Quan A, et al. Poly(ε-Caprolactone) nanofiber wrap improves nerve regeneration and functional outcomes after delayed nerve repair. *Plas Reconst Surg*. 2019;144(1):48e–57e. doi:10.1097/PRS.0000000000005715
22. Yen CM, Shen CC, Yang YC, et al. Novel electrospun poly(ε-caprolactone)/type I collagen nanofiber conduits for repair of peripheral nerve injury. *Neural Regen Res*. 2019;14(9):1617–1625. doi:10.4103/1673-5374.255997
23. Wang J, Zheng W, Chen L, et al. Enhancement of Schwann cells function using graphene-oxide-modified nanofiber scaffolds for peripheral nerve regeneration. *ACS Biomater Sci Eng*. 2019;5:2444–2456. doi:10.1021/acsbiomaterials.8b01564
24. Neshat A, Nazarpak MH, Mansoori K, et al. Bilayer cylindrical conduit consisting of electrospun polycaprolactone nanofibers and DSC cross-linked sodium alginate hydrogel to bridge peripheral nerve gaps. *Macromol Biosci*. 2020;20:2000149. doi:10.1002/mabi.202000149
25. Wang J, Xiong H, Zhu T, et al. Bioinspired multichannel nerve guidance conduit based on shape memory nanofibers for potential application in peripheral nerve repair. *ACS Nano*. 2020;14(10):12579–12595. doi:10.1021/acsnano.0c03570
26. Zhang Q, Tong Z, Chen F, et al. Aligned soy protein isolate-modified poly(L-lactic acid) nanofibrous conduits enhanced peripheral nerve regeneration. *J Neural Eng*. 2020;17:036003. doi:10.1088/1741-2552/ab8d81
27. Moharrami Kasmaie F, Zamani F, Sayad-Fathi S, Zaminy A. Promotion of nerve regeneration by biodegradable nanofibrous scaffold following sciatic nerve transection in rats. *Prog Biomater*. 2021;10:53–64. doi:10.1007/s40204-021-00151-w
28. Niu Y, Stadler FJ, Fu M. Biomimetic electrospun tubular PLLA/gelatin nanofiber scaffold promoting regeneration of sciatic nerve transection in SD rat. *Mater Sci Eng C Mater Biol Appl*. 2021;121:111858. doi:10.1016/j.msec.2020.111858
29. Zheng C, Yang Z, Chen S, et al. Nanofibrous nerve guidance conduits decorated with decellularized matrix hydrogel facilitate peripheral nerve injury repair. *Theranostics*. 2021;11(6):2917–2931. doi:10.7150/thno.50825
30. Kaka G, Arum J, Sadraie SH, Emamgholi A, Mohammadi A. Bone marrow stromal cells associated with poly l-lactic-co-glycolic acid (PLGA) nanofiber scaff old improve transected sciatic nerve regeneration. *Iranian J Biotech*. 2017;15(3):e1576. doi:10.15171/ijb.1576

31. Hu F, Zhang X, Liu H, et al. Neuronally differentiated adipose-derived stem cells and aligned PHBV nanofiber nerve scaffolds promote sciatic nerve regeneration. *Biochem Biophy Res Commun*. 2017;489:171–178. doi:10.1016/j.bbrc.2017.05.119
32. Das S, Sharma M, Saharia D, Sarma KK, Muir EM, Bora U. Electrospun silk-polyaniline conduits for functional nerve regeneration in rat sciatic nerve injury model. *Biomed Mater*. 2017;12:045025. doi:10.1088/1748-605X/aa7802
33. Farzamfar S, Ehterami A, Salehi M, Vaeez A, Atashi A, Sahrapeyma H. Unrestricted somatic stem cells loaded in nanofibrous conduit as potential candidate for sciatic nerve regeneration. *J Mol Neurosci*. 2019;67:48–61. doi:10.1007/s12031-018-1209-9
34. Pereira Dos Santos FP, Peruch T, Katami SJV, et al. Poly (lactide-co-glycolide) (PLGA) scaffold induces short-term nerve regeneration and functional recovery following sciatic nerve transection in rats. *Neuroscience*. 2018;396:94–107. doi:10.1016/j.neuroscience.2018.11.007
35. Ma T, Yang Y, Quan X, et al. Oxygen carrier in core-shell fibers synthesized by coaxial electrospinning enhances Schwann cell survival and nerve regeneration. *Theranostics*. 2020;10(20):8957–8973. doi:10.7150/thno.45035
36. Suzuki K, Tanaka H, Ebara M, et al. Electrospun nanofiber sheets incorporating methylcobalamin promote nerve regeneration and functional recovery in a rat sciatic nerve crush injury model. *Acta Biomater*. 2017;53:250–259. doi:10.1016/j.actbio.2017.02.004
37. Chang YC, Chen MH, Liao SY, et al. Multi-channeled nerve guidance conduit with spatial gradients of neurotrophic factors and oriented nanotopography for repairing the peripheral nervous system. *ACS Appl Mater Interfaces*. 2017;9(43):37623–37636. doi:10.1021/acsami.7b12567
38. Naseri-Nosar M, Salehi M, Hojjati-Emami S. Cellulose acetate/poly lactic acid coaxial wet-electrospun scaffold containing citalopram-loaded gelatin nanocarriers for neural tissue engineering applications. *Int J Biol Macromol*. 2017;103:701–708. doi:10.1016/j.ijbiomac.2017.05.054
39. Hong MH, Hong HJ, Pang H, Lee HJ, Yi S, Koh WG. Controlled release of growth factors from multi-layered fibrous scaffold for functional recoveries in crushed sciatic nerve. *ACS Biomater Sci Eng*. 2018;4(2):576–586. doi:10.1021/acsbiomaterials.7b00801
40. Farzamfar S, Naseri-Nosar M, Vaez A, et al. Neural tissue regeneration by a gabapentin-loaded cellulose acetate/gelatin wet-electrospun scaffold. *Cellulose*. 2018;25:1229–1238. doi:10.1007/s10570-017-1632-z
41. Xia B, Lv Y. Dual-delivery of VEGF and NGF by emulsion electrospun nanofibrous scaffold for peripheral nerve regeneration. *Mater Sci Eng C Mater Biol Appl*. 2018;82:253–264. doi:10.1016/j.msec.2017.08.030
42. Cheong H, Kim J, Kim BJ, et al. Multi-dimensional bioinspired tactics using an engineered mussel protein glue-based nanofiber conduit for accelerated functional nerve regeneration. *Acta Biomater*. 2019;90:87–99. doi:10.1016/j.actbio.2019.04.018
43. Sayanagi J, Tanaka H, Ebara M, et al. Combination of electrospun nanofiber sheet incorporating methylcobalamin and PGA-collagen tube for treatment of a sciatic nerve defect in a rat model. *J Bone Joint Surg Am*. 2020;102(3):245–253. doi:10.2106/JBJS.19.00254
44. Rao F, Wang Y, Zhang D, et al. Aligned chitosan nanofiber hydrogel grafted with peptides mimicking bioactive brain-derived neurotrophic factor and vascular endothelial growth factor repair long-distance sciatic nerve defects in rats. *Theranostics*. 2020;10(4):1590–1603. doi:10.7150/thno.36272
45. Chen X, Ge X, Qian Y, et al. Electrospinning multilayered scaffolds loaded with melatonin and Fe3O4 magnetic nanoparticles for peripheral nerve regeneration. *Adv Funct Mater*. 2020;30:2004537. doi:10.1002/adfm.202070258
46. Amini S, Saudi A, Amirpour N, et al. Application of electrospun polycaprolactone fibers embedding lignin nanoparticle for peripheral nerve regeneration: in vitro and in vivo study. *Int J Bio Macromol*. 2020;159:154–173. doi:10.1016/j.ijbiomac.2020.05.073
47. Samadian H, Ehterami A, Sarrafzadeh A, et al. Sophisticated polycaprolactone/gelatin nanofibrous nerve guided conduit containing platelet-rich plasma and citicoline for peripheral nerve regeneration: in vitro and in vivo study. *Int J Bio Macromol*. 2020;150:380–388. doi:10.1016/j.ijbiomac.2020.02.102
48. Jahromi HK, Farzin A, Hasanzadeh E, et al. Enhanced sciatic nerve regeneration by poly-L-lactic acid/multi-wall carbon nanotube neural guidance conduit containing Schwann cells and curcumin encapsulated chitosan nanoparticles in rat. *Mater Sci Eng C Mater Biol Appl*. 2020;109:110564. doi:10.1016/j.msec.2019.110564
49. Zhou G, Chang W, Zhou X, et al. Nanofibrous nerve conduits with nerve growth factors and bone marrow stromal cells pre-cultured in bioreactors for peripheral nerve regeneration. *ACS Appl Mater Interfaces*. 2020;12:16168–16177. doi:10.1021/acsami.0c04191
50. Jahromi M, Razavi S, Seyedebrahimi R, Reisi P, Kazemi M. Regeneration of rat sciatic nerve using PLGA conduit containing rat ADSCs with controlled release of BDNF and gold nanoparticles. *J Mol Neurosci*. 2021;71:746–760. doi:10.1007/s12031-020-01694-6
51. Mondal D, Griffith M, Venkatraman SS. Polycaprolactone-based biomaterials for tissue engineering and drug delivery: current scenario and challenges. *Int J Polym Mater Polym Biomater*. 2016;65(5):255–265. doi:10.1080/00914037.2015.1103241
52. Duek EAR, Zavaglia CAC, Belangero WD. In vitro study of poly (lactic acid) pin degradation. *Polymer*. 1999;40:6465–6473. doi:10.1016/S0032-3861(98)00846-5
53. Ma T, Wang Y, Qi F, et al. The effect of synthetic oxygen carrier-enriched fibrin hydrogel on Schwann cells under hypoxia condition in vitro. *Biomaterials*. 2013;34:10016–10027. doi:10.1016/j.biomaterials.2013.09.047
54. Bao M, Wang X, Yuan H, Lou X, Zhao Q, Zhang Y. HAp incorporated ultrafine polymeric fibers with shape memory effect for potential use in bone screw hole healing. *J Mater Chem B*. 2016;4(31):5308–5320. doi:10.1039/c6tb01305h
55. Cha HJ, Hwang DS, Lim S. Development of bioadhesives from marine mussels. *Biotechnol J*. 2008;3(5):631–638. doi:10.1002/biot.200700258
56. Borschel GH, Kia KF, Kuzon WM, Dennis RG. Mechanical properties of acellular peripheral nerve. *J Surg Res*. 2003;114(2):133–139. doi:10.1016/s0022-4804(03)00255-5
57. Sudwilai T, Ng JJ, Boonkrai C, Israsena N, Chuangchote S, Supaphol P. Polypyrrole-coated electrospun poly(lactic acid) fibrous scaffold: effects of coating on electrical conductivity and neural cell growth. *J Biomater Sci Polym Ed*. 2014;25(12):1240–1252. doi:10.1080/09205063.2014.926578
58. Huang J, Lu L, Zhang J, et al. Electrical stimulation to conductive scaffold promotes axonal regeneration and remyelination in a rat model of large nerve defect. *PLoS One*. 2012;7:e39526. doi:10.1371/journal.pone.0039526
59. Sulaiman OR, Gordon T. A rat study of the use of end-to-side peripheral nerve repair as a "babysitting" technique to reduce the deleterious effect of chronic denervation. *J Neurosurg*. 2019;131:622–632. doi:10.3171/2018.3.JNS172357
60. Peng J, Wang Y, Zhang L, et al. Human umbilical cord Wharton's jelly-derived mesenchymal stem cells differentiate into a Schwann-cell phenotype and promote neurite outgrowth in vitro. *Brain Res Bull*. 2011;84(3):235–243. doi:10.1016/j.brainresbull.2010.12.013
61. Usach V, Coronel F, Malet M, et al. Bone marrow-derived cells and peripheral nerve injury: translational implications for pain and regeneration treatments. *Clin Pharmacol Transl Med*. 2018;2(2):112–124.

62. Neo WH, Yap K, Lee SH, et al. MicroRNA miR-124 controls the choice between neuronal and astrocyte differentiation by fine-tuning Ezh2 expression. *J Biol Chem*. 2014;289:20788–20801. doi:10.1074/jbc.M113.525493
63. Hu F, Sun B, Xu P, et al. MiR-218 induces neuronal differentiation of ASCs in a temporally sequential manner with fibroblast growth factor by regulation of the wnt signaling pathway. *Sci Rep*. 2017;7:39427. doi:10.1038/srep39427
64. Murray-Dunning C, McArthur SL, Sun T, McKean R, Ryan AJ, Haycock JW. Three-dimensional alignment of Schwann cells using hydrolysable microfiber scaffolds: strategies for peripheral nerve repair. *Methods Mol Biol*. 2011;695:155–166. doi:10.1007/978-1-60761-984-0_10
65. Liu F, Xuan A, Chen Y, et al. Combined effect of nerve growth factor and brain-derived neurotrophic factor on neuronal differentiation of neural stem cells and the potential molecular mechanisms. *Mol Med Rep*. 2014;10(4):1739–1745. doi:10.3892/mmr.2014.2393
66. Chan JR, Cosgaya JM, Wu YJ, Shooter EM. Neurotrophins are key mediators of the myelination program in the peripheral nervous system. *Proc Natl Acad Sci U S A*. 2001;98(25):14661–14668. doi:10.1073/pnas.251543398
67. Sofroniew MV, Howe CL, Mobley WC. Nerve growth factor signaling, neuroprotection, and neural repair. *Annu Rev Neurosci*. 2001;24:1217–1281. doi:10.1146/annurev.neuro.24.1.1217
68. Tuszynski MH, Blesch A. Nerve growth factor: from animal models of cholinergic neuronal degeneration to gene therapy in Alzheimer's disease. *Prog Brain Res*. 2004;146:441–449. doi:10.1016/s0079-6123(03)46028-7
69. Bhang SH, Lee TJ, Yang HS, et al. Enhanced nerve growth factor efficiency in neural cell culture by immobilization on the culture substrate. *Biochem Biophys Res Commun*. 2009;382(2):315–320. doi:10.1016/j.bbrc.2009.03.016
70. Lee AC, Yu VM, Lowe JB, et al. Controlled release of nerve growth factor enhances sciatic nerve regeneration. *Exp Neurol*. 2003;184(1):295–303. doi:10.1016/s0014-4886(03)00258-9
71. Grill R, Murai K, Blesch A, Gage FH, Tuszynski MH. Cellular delivery of neurotrophin-3 promotes corticospinal axonal growth and partial functional recovery after spinal cord injury. *J Neurosci*. 1997;17(14):5560–5572. doi:10.1523/JNEUROSCI.17-14-05560.1997
72. Horner PJ, Gage FH. Regenerating the damaged central nervous system. *Nature*. 2000;407(6807):963–970. doi:10.1038/35039559
73. Namiki J, Kojima A, Tator CH. Effect of brain-derived neurotrophic factor, nerve growth factor, and neurotrophin-3 on functional recovery and regeneration after spinal cord injury in adult rats. *J Neurotrauma*. 2000;17(12):1219–1231. doi:10.1089/neu.2000.17.1219
74. Erlandsson A, Enarsson M, Forsberg-Nilsson K. Immature neurons from CNS stem cells proliferate in response to platelet-derived growth factor. *J Neurosci*. 2001;21(10):3483–3491. doi:10.1523/JNEUROSCI.21-10-03483.2001
75. Kawabe T, Wen TC, Matsuda S, Ishihara K, Otsuda H, Sakanaka M. Platelet-derived growth factor prevents ischemia-induced neuronal injuries in vivo. *Neurosci Res*. 1997;29(4):335–343. doi:10.1016/s0168-0102(97)00105-3
76. Verheyen A, Peeraer E, Lambrechts D, et al. Therapeutic potential of VEGF and VEGF-derived peptide in peripheral neuropathies. *Neuroscience*. 2013;244:77–89. doi:10.1016/j.neuroscience.2013.03.050
77. Sondell M, Lundborg G, Kanje M. Vascular endothelial growth factor stimulates Schwann cell invasion and neovascularization of acellular nerve grafts. *Brain Res*. 1999;846(2):219–228. doi:10.1016/s0006-8993(99)02056-9
78. Ren Q, Ye S, Whiteheart SW. The platelet release reaction: just when you thought platelet secretion was simple. *Curr Opin Hematol*. 2008;15(5):537–541. doi:10.1097/MOH.0b013e328309ec74
79. Agrawal AA. Evolution, current status and advances in application of platelet concentrate in periodontics and implantology. *World J Clin Cases*. 2017;5(5):159–171. doi:10.12998/wjcc.v5.i5.159
80. Choi BH, Choi YS, Kang DG, Kim BJ, Song YH, Cha HJ. Cell behavior on extracellular matrix mimic materials based on mussel adhesive protein fused with functional peptides. *Biomaterials*. 2010;31(34):8980–8988. doi:10.1016/j.biomaterials.2010.08.027
81. Hwang DS, Gim Y, Yoo HJ, Cha HJ. Practical recombinant hybrid mussel bioadhesive fp-151. *Biomaterials*. 2007;28(24):3560–3568. doi:10.1016/j.biomaterials.2007.04.039
82. Huelsenbeck SC, Rohrbeck A, Handreck A, et al. C3 peptide promotes axonal regeneration and functional motor recovery after peripheral nerve injury. *Neurotherapeutics*. 2012;9(1):185–198. doi:10.1007/s13311-011-0072-y
83. Lu J, Sun X, Yin H, Shen X, Yang S, Wang Y. A neurotrophic peptide-functionalized self-assembling peptide nanofiber hydrogel enhances rat sciatic nerve regeneration. *Nano Res*. 2018;11:4599–4613. doi:10.1007/s12274-018-2041-9
84. Liu X, Wang X, Horii A, et al.. In vivo studies on angiogenic activity of two designer self-assembling peptide scaffold hydrogels in the chicken embryo chorioallantoic membrane. *Nanoscale*. 2012;4(8):2720–2727. doi:10.1039/c2nr00001f
85. Akaike A, Tamura Y, Sato Y, Yokota T. Protective effects of a vitamin B12 analog, methylcobalamin, against glutamate cytotoxicity in cultured cortical neurons. *Eur J Pharmacol*. 1993;241(1):1–6. doi:10.1016/0014-2999(93)90925-8
86. Okada K, Tanaka H, Temporin K, et al. Methylcobalamin increases Erk1/2 and Akt activities through the methylation cycle and promotes nerve regeneration in a rat sciatic nerve injury model. *Exp Neurol*. 2010;222(2):191–203. doi:10.1016/j.expneurol.2009.12.017
87. Hashimoto S, Inoue T, Muraki I, Koyama T. Effects of acute citalopram on the expression of conditioned freezing in naive versus chronic citalopram-treated rats. *Prog Neuropsychopharmacol Biol Psychiatry*. 2009;33(1):113–117. doi:10.1016/j.pnpbp.2008.10.015
88. Verdi J, Mortazavi-Tabatabaei SA, Sharif S, Verdi H, Shoae-Hassani A. Citalopram increases the differentiation efficacy of bone marrow mesenchymal stem cells into neuronal-like cells. *Neural Regen Res*. 2014;9(8):845–850. doi:10.4103/1673-5374.131601
89. Rosa AS, Freitas MF, Rocha IR, Chacur M. Gabapentin decreases microglial cells and reverses bilateral hyperalgesia and allodynia in rats with chronic myositis. *Eur J Pharmacol*. 2017;799:111–117. doi:10.1016/j.ejphar.2017.02.012
90. Câmara CC, Araújo CV, de Sousa KKO, et al. Gabapentin attenuates neuropathic pain and improves nerve myelination after chronic sciatic constriction in rats. *Neurosci Lett*. 2015;607:52–58. doi:10.1016/j.neulet.2015.09.021
91. Benga A, Zor F, Korkmaz A, Marinescu B, Gorantla V. The neurochemistry of peripheral nerve regeneration. *Indian J Plast Surg*. 2017;50(1):5–15. doi:10.4103/ijps.IJPS_14_17
92. Altunkaynak BZ, Delibas B, Altun G, Deniz OG. Melatonin and sciatic nerve injury repair: a current perspective. *J Neurorestoratol*. 2017;55:49–60. doi:10.2147/JN.S140614
93. Noori Hassanvand M, Soleimani Mehranjani M, Shojafar E. Melatonin improves the structure and function of autografted mice ovaries through reducing inflammation: a stereological and biochemical analysis. *Int Immunopharmacol*. 2019;74:105679. doi:10.1016/j.intimp.2019.105679
94. Saudi A, Amini S, Amirpour N, et al. Promoting neural cell proliferation and differentiation by incorporating lignin into electrospun poly(vinyl alcohol) and poly(glycerol sebacate) fibers. *Mater Sci Eng C Mater Biol Appl*. 2019;104:110005. doi:10.1016/j.msec.2019.110005

95. Gareri P, Castagna A, Cotroneo AM, Putignano S, De Sarro G, Bruni AC. The role of citicoline in cognitive impairment: pharmacological characteristics, possible advantages, and doubts for an old drug with new perspectives. *Clin Interv Aging*. 2015;10:1421–1429. doi:10.2147/CIA.S87886
96. Barrachina M, Domínguez I, Ambrosio S, Secades J, Lozano R, Ferrer I. Neuroprotective effect of citicoline in 6-hydroxydopamine-lesioned rats and in 6-hydroxydopamine-treated SH-SY5Y human neuroblastoma cells. *J Neurol Sci*. 2003;215(1–2):105–110. doi:10.1016/s0022-510x(03)00204-1
97. Ma J, Liu J, Yu H, Wang Q, Chen Y, Xiang L. Curcumin promotes nerve regeneration and functional recovery in rat model of nerve crush injury. *Neurosci Lett*. 2013;547:26–31. doi:10.1016/j.neulet.2013.04.054
98. Noorafshan A, Omidi A, Karbalay-Doust S, Aliabadi E, Dehghani F. Effects of curcumin on the dorsal root ganglion structure and functional recovery after sciatic nerve crush in rat. *Micron*. 2011;42(5):449–455. doi:10.1016/j.micron.2011.01.002
99. Velasquez JT, Nazareth L, Quinn RJ, Ekberg JAK, St. John JA. Stimulating the proliferation, migration and lamellipodia of Schwann cells using low-dose curcumin. *Neuroscience*. 2016;324:140–150. doi:10.1016/j.neuroscience.2016.02.073
100. Khajavi M, Shiga K, Wiszniewski W, et al. Oral curcumin mitigates the clinical and neuropathologic phenotype of the Trembler-J mouse: a potential therapy for inherited neuropathy. *Am J Hum Genet*. 2007;81(3):438–453. doi:10.1086/519926
101. Giannaccini M, Calatayud MP, Poggetti A, et al. Magnetic nanoparticles for efficient delivery of growth factors: stimulation of peripheral nerve regeneration. *Adv Healthc Mater*. 2017;6(7):1601429. doi:10.1002/adhm.201601429
102. Kim JA, Lee N, Kim BH, et al. Enhancement of neurite outgrowth in PC12 cells by iron oxide nanoparticles. *Biomaterials*. 2011;32 (11):2871–2877. doi:10.1016/j.biomaterials.2011.01.019
103. Razavi S, Seyedebrahimi R, Jahromi M. Biodelivery of nerve growth factor and gold nanoparticles encapsulated in chitosan nanoparticles for Schwann-like cells differentiation of human adipose-derived stem cells. *Biochem Biophys Res Commun*. 2019;513(3):681–687. doi:10.1016/j.bbrc.2019.03.189
104. Tang SY, Sivakumar M, Ng AM, Shridharan P. Anti-inflammatory and analgesic activity of novel oral aspirin-loaded nanoemulsion and nano multiple emulsion formulations generated using ultrasound cavitation. *Intern J Pharm*. 2012;430:299–306. doi:10.1016/j.ijpharm.2012.03.055
105. Xu X, Wang S, Wu H, Liu Y, Xu F, Zhao J. A multimodal antimicrobial platform based on MXene for treatment of wound infection. *Colloids Surf B Biointerfaces*. 2021;207:111979. doi:10.1016/j.colsurfb.2021.111979
106. Qian Y, Wang X, Song J, Chen W, Chen S, Jin Y. Preclinical assessment on neuronal regeneration in the injury-related microenvironment of graphene-based scaffolds. *NPJ Regen Med*. 2021;6(1):31. doi:10.1038/s41536-021-00142-2
107. Qian Y, Xu Y, Yan Z, et al. Boron nitride nanosheets functionalized channel scaffold favors microenvironment rebalance cocktail therapy for piezocatalytic neuronal repair. *Nano Energy*. 2021;83:105779. doi:10.1016/j.nanoen.2021.105779
108. Fadia NB, Bliley JM, DiBernardo GA, et al. Long-gap peripheral nerve repair through sustained release of a neurotrophic factor in nonhuman primates. *Sci Transl Med*. 2020;12(527):eaav7753. doi:10.1126/scitranslmed.aav7753